Volume 4, Issue 1, June 2020

ISSN 2587-1943

IJIEA

INTERNATIONAL JOURNAL OF INNOVATIVE ENGINEERING APPLICATIONS

International Journal of Innovative Engineering Applications is published June and December.

Adress for the manuscripts and correspondence:
Uluslararası Yenilikçi Mühendislik Uygulamaları Dergisi
Fırat Üniversitesi Kampüsü, Teknoloji Fakültesi, Merkez–Elazığ

Tel: +90 424 237 0000/ Ext.7655
e-mail: ijieatr@gmail.com

ISSN: 2587-1943

Elazığ-2020

IJIEA

IJIEA
volume 4 issue 1

İÇİNDEKİLER

IJIEA

International Journal of Innovative Engineering Applications

Journal homepage: https://dergipark.org.tr/ijiea

EFFECT OF DYNAMIC VISCOSITY ON NANOFIBER DIAMETERS AND ELECTRICAL CONDUCTIVITY OF POLYACRYLONITRILE NANOFIBERS DOPED NANO-CU PARTICLES

Olivier M. Mpukuta[1], Kevser Dincer*[1], İlkay Özaytekin[1]

[1]*Konya Technical University, Engineering and Natural Sciences Faculty, Department of Mechanical Engineering, Turkey*

Abstract

Original scientific paper

In this study, pure polyacrylonitrile (PAN) nanofibers in the diameter range of 200-500 nm and PAN/Cu composite nanofibers in 200-600 nm diameter range were produced at applied voltage of 15 kV. The distribution of fiber diameters, the dynamic viscosities of the solutions and the electrical conductivity (EC) of the produced fibers were examined as a function of copper nanoparticles content (1%, 3% and 5% by weight). The dynamic viscosity of the electrospinning solution was an important parameter on the nanofiber morphology as well as on the nanofiber diameter distribution. Taken together, the data analysis showed that the highest EC value was $38x10^{-2}$ S/cm, which was obtained from nanofibers produced by electrospinning solution containing %1 Cu nanoparticle having a dynamic viscosity value of 577.7 mPa.s. The addition of Cu nanoparticles increased the EC of pure PAN nanofibers by a factor of 2.37. In addition, further analysis of pure PAN nanofibers and %1 Cu/PAN nanofibers were performed by XRD, contact angle and TGA devices. Results showed that the TGA degradation curves of both pure PAN and Cu-based PAN nanofibers presented the same behavior. In DSC analysis, the glass transition temperature of pure PAN nanofibers was observed at 112 °C, while no glass transition temperature was observed for PAN nanofibers containing 1% Cu.

Keywords: *Copper nanoparticles, Electrical conductivity, Electrospinning, Nanofibers, Thermal stability*

1 Introduction

Nowadays, fabrication of nanofibers containing nanoparticles is attracting widespread interest due to the fact that the resultant composite fibers take advantage of the outstanding properties of each component [1-3]. Nanofibers have very fine diameters and perfect pore interconnectivity. For this reason, they have extremely high specific surface area and porous structure. Composite nanofibers may provide solutions to both technological and environmental areas, such as solar energy conversion, electronic, filtration, protective textiles, biotechnology, biomedical sciences and so on [3, 4].

General production techniques such as drawing, phase separation, self-assembly, template synthesis, chemical vapor deposition, wet chemical synthesis and electrospinning have been used in the production of nanofibers in recent years [5]. It is worth noting that, among these methods, electrospinning has been studied widely because of its efficiency, simplicity, low cost and allows the preparation of continuous fibers with diameters down to a few nanometers as well [4, 6, 7]. What is more, various one-dimensional nanostructured materials such as metals, metal oxides, hydrocarbons, composites and so forth can be fabricated by electrospinning process [7]. Electrospinning is fundamentally different from air or other mechanically driven spinning techniques in that the extrusion force is a consequence of the interaction between the external applied electric field and the charged polymer [8]. The phenomenon is such as a high voltage applied on the solution leads to a highly charged polymer fluid, which in its turn allows the solution droplet at the tip to experience two main types of forces, the surface tension and the electrostatic repulsion force. When the charges in the solution reach the critical amount, an elongated cone called Taylor cone will be formed with the effect of its voltage. If the threshold voltage is above, an electrospinning jet is emitted. As the tension increases, the micro-dripping and intermittent jet becomes the Taylor cone jet. The electrospinning jet will travel towards the region of lower potential referred as collector and becomes narrower in the process [8, 9]. Although the setup for electrospinning looks extremely simple, the physics behind it is very complex and involves the understanding of some notions such as fluid rheology, electrostatics and polymer solution [9]. The electrospinning process is controlled by many parameters, which can influence the transformation of polymer solutions into nanofibers. These parameters are mainly consisted of three categories: solutions parameters, governing variables and ambient parameters. Solution parameters include viscosity, conductivity, molecular weight, molecular weight distribution, elasticity, and surface tension. Process parameters include electric potential at the capillary tip, hydrostatic pressure in the capillary tube, flow rate and concentration, and the gap (distance between the tip and the collecting screen). Ambient parameters include temperature, humidity, and the air velocity in the electrospinning chamber [5, 8, 10]. It was reported that since all these parameters significantly

* Corresponding author.

E-mail address: kdincer@ktun.edu.tr (K. Dinçer) | ORCID Number : 0000-0001-6681-5294

Received 21 March 2020; Received in revised form 9 June 2020; Accepted 20 June 2020

 Doi: https://doi.org/10.46460/ijiea.707142

affect the morphology and structure of the as-spun nanofibers, it is possible to obtain nanofibers with the desired diameter and morphology by controlling these parameters [8, 11]. For instance, it was reported that the viscoelasticity of the solution, charge density carried by the jet, and the surface tension of the solution are the key factors that influence the formation of the beaded fibers. The increase in viscosity only supports bead-free fiber formation, while the increase in net charge density supports both bead-free fiber formation and finer fiber formation. Reducing surface tension also promotes bead-free fiber formation [12]. Another statement is fibers with a finer diameter can be obtained by reducing the concentration of the polymer in the solution [13].

In recent years, different combinations of polyacrylonitrile (PAN) polymers and nanoparticles were used to fabricate composite nanofibers for different purposes. Among them, PAN/ SiO_2, PAN/TiO_2 and PAN/Bi_2O_3 electrospun nanofibers were fabricated and their physical properties were examined [14], PAN/$AgNO_3$ were used to prepare fibrous membranes with antibacterial activity [15], PAN/ZnO and PAN/Fe_2O_3 nanofibers have been used to detect carbon dioxide [16]. It was reported that by using PAN nanofibers coated with a thin layer of conjugated polymer it was possible to detect explosive 2, 4, 6- trinitrotoluene (TNT) vapor [17, 18] and so on. But to the best of our knowledge, there is a lack of significant studies on EC of electrospun PAN fibers containing copper nanoparticles in the open literature. Therefore, in this study, the effect of dynamic viscosity of Cu-based electrospinning solutions on the diameter and EC of the produced fibers has been investigated. Thermal degradation, surface contact angle and crystallinity structure of PAN nanofibers of the highest EC value were also performed. The produced materials can be used for various applications such as sensor devices, solar cells, PEM fuel cells and so on.

2 Experimental

2.1 Materials

Polyacrylonitrile powder (PAN, Mw=150,000g/mol) and N, N- Dimethylformamide anhydrous, (DMF, 99.8 %) were purchased from Sigma-Aldrich Co. Copper (Cu, 25 nm, 99.9 %) was provided from Nanografi Co. Ltd. The chemicals provided in this study were used without purification.

2.2 Fabrication of pure PAN and PAN/Cu Nanofibers

The obtained solutions were stirred in the similar conditions as it has been done for pure PAN solutions. Finally, the solutions were poured into syringes. The following Figure 1 illustrate the procedure of the electrospinning solutions preparation.

The electrospinning setup consisted of a syringe pump, nanofiber collector and a power supply. The solution was held in a horizontal syringe with a stainless steel needle. The stainless steel needle was connected to an electrically positive high voltage power supply, while the metallic disk used as the fiber collector was connected to an electrically the negative high voltage power supply. For electrospinning, the distance between the collector and the needle was set to 12 cm. The volumetric flow rate of the solution was maintained at 2.5 mL/h using a digitally controlled syringe pump for each copper content in solutions of nanofibers were performed at 15 kV.

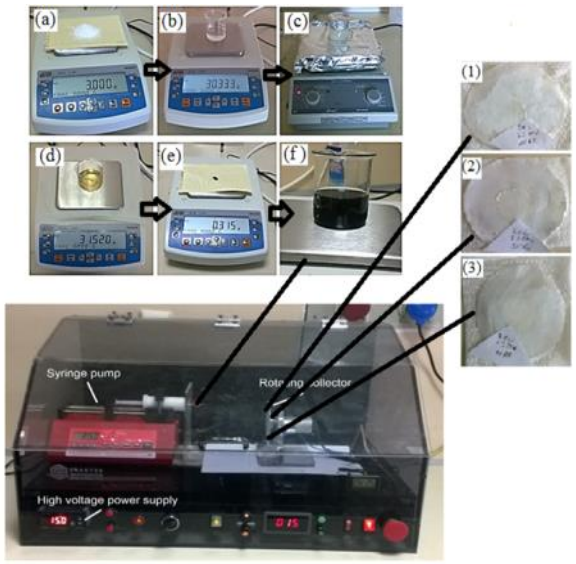

Figure 1. Preparation electrospinning solution for PAN nanofibers with CuNPs (a) PAN, (b) DMF, (c) Steering of PAN/DMF mixture, (d) PAN/DMF solutions after steering, (e) CuNPs (f) mixture of PAN/DMF/CuNPs after steering process (1) PAN nanofibers with 1 wt % CuNPs (2) PAN nanofibers with 3 wt % CuNPs (3) PAN nanofibers with 5 wt % CuNPs

In this study, two categories of solutions (pure PAN solutions and PAN/CuNPs solutions) were prepared. Firstly, 9 wt. % of PAN was dissolved in DMF and stirred using a magnetic stirrer device at 85°C and 1200 rpm for an hour so as to obtain homogenized solutions. The solutions were designated as pure PAN solutions in this paper. In the second category, the copper nanoparticles (1, 3 and 5 wt. %) was added into the previous PAN/DMF solutions, respectively.

2.3 Characterization of nanofibers

For SEM analysis of nanofibers produced from four different PAN solutions, the nanofibers were first coated with a thin gold layer by electrodeposition method and then the nanofibers were examined using SM Zeiss LS-10 microscope. XRD analysis was measured from 10° to 90° for 2θ and at the scanning speed of 5°/min with a Bruker D8 X-ray diffractometer equipped with a Cu Kα anode (λ=1.541 Å). The contact angle measurement device (Dataphysics instruments GmbH, model OCA15 Pro, version 1.3) was used to analyze the hydrophobicity of nanocomposites fibers. To do so, a dosing volume of 2 µL of water was used at 0.5 µL/s as dosing rate. Thermal

degradation of PAN and PAN doped 1 wt.% copper nanofibers up to 900℃ was investigated by TGA analysis. For this, the nanofibers were heated at 0 - 900 ° C with a heating rate of 10 ° C/min in a nitrogen atmosphere. EC values of PAN and PAN doped 1 wt.% copper nanofibers were measured using a four point probe device (ENTEK Elk. FPP-460 with Pt probes) at room temperature. The glass translation temperatures, crystallization peak temperatures and melting point temperature of PAN and PAN doped 1 wt.% copper nanofibers were determined by DSC analysis.

3 Results and Discussion

The scanning electron microscopy (SEM) was performed to examine the morphology of the as-spun nanofibers). Figure 2 presents the SEM images and the graphs of nanofiber diameter distribution of the as-spun pure PAN fibers and PAN/Cu fibers with different copper nanoparticles percentage of mass contents (1, 3 and 5 wt. %) produced at 15 kV, respectively. As can be seen in the Figure 2, taken together by adding copper nanoparticles in the electrospinning solution did not affect negatively the morphology of the as-spun composite nanofibers. Like in the case of pure PAN solutions, most of electrospinning solutions containing copper nanoparticles had the fabrication of beads-free and uniform composite fibers. However, for the fibers obtained with electrospinning solution containing 1 % Cu, homogeneous fibers with a narrower diameter distribution were found to be closer to each other. As the copper concentration in the solution increased, the diameter distribution ranges increased and fibers with different diameters were obtained. In addition, no agglomeration of copper nanoparticles was observed on the surface of the nanofibers. When the diameter of PAN/Cu nanofibers were compared to that of pure PAN nanofibers, it was determined that PAN nanofiber average diameter containing 1% Cu had the lowest and most homogeneous diameter distribution. In this study the average diameters of fibers were 327.19 nm for pure PAN fibers and 271 nm, 362.5 nm and 306.26 nm for PAN/Cu nanofibers containing 1, 3 and 5 wt. % of copper nanoparticles, respectively. A rotational viscometer (JK-RV-1) was used to analyze the viscosity of the electrospinning solutions with and without copper nanoparticles. The dynamic viscosity of the solutions (also known as absolute viscosity) was found to be 462.5 mPa.s for pure PAN (9 wt. %) and 577.7, 3160.25 and 11526.66 mPa.s for electrospinning solutions containing 1, 3 and 5 wt. % Cu, respectively. As can be seen in Figure 3a-c, the marked observation to emerge from the graph investigation is that the viscosity of the solutions increased with an increase of copper nanoparticles contents. As expected, nanofibers with more uniform distribution were obtained with an increase of dynamic viscosity. However, in this study, the diameter distribution was non-uniform when more than 1% Cu was added [19]. Figure 3b reports the variation of the mean diameter distributions of nanofiber against the dynamic viscosity of the solution. In this study the average diameters of fibers were 327.19 nm for pure PAN fibers and 271 nm, 362.5 nm.

The EC of the pure PAN fibers and fibers containing copper nanoparticles was examined by using the four-point probe technique. The results are compared in Figure 3a. The EC values were 5.81×10^{-3} S/cm for pure PAN nanofibers and 1.38×10^{-2}, 8.69×10^{-2} and 4.43×10^{-3} S/cm for nanofibers containing (1, 3 and 5 wt. %) of copper nanoparticles percentage of nanofiber mass contents, respectively. As can be seen in Figure 3, higher EC were obtained at low copper nanoparticles contents (1 wt. %). It is worth noting that PAN nanofibers with 1 wt. % of copper performed at 15 kV present a 137.52 % increase in the value of EC compared to pure PAN nanofibers. However, in 5 wt. % of copper nanoparticles contents, nanofibers presented an EC lower than that of pure PAN nanofibers. Results show that the EC value decreases beyond the dynamic viscosity value of 577.7 mPa.s. Therefore, in this study, the dynamic viscosity value of 577.7 mPa.s could be taken as the optimum dynamic viscosity value for EC of PAN fibers containing copper nanoparticles.

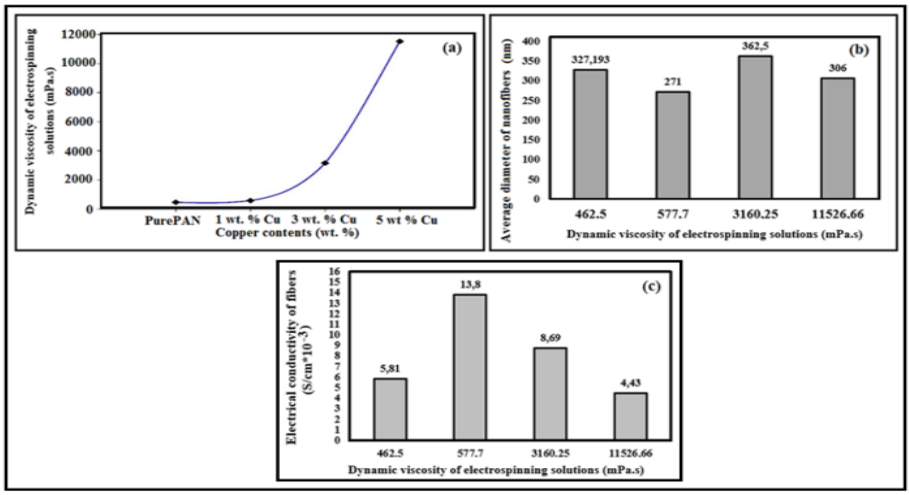

Figure 2. SEM images and diameter distributions of pure PAN and PAN nanofibers with Cu (a) pure PAN nanofibers (b) PAN nanofibers with 1 wt % Cu, (c) PAN nanofibers with 3 wt % Cu, (d) PAN nanofibers with 5 wt % Cu

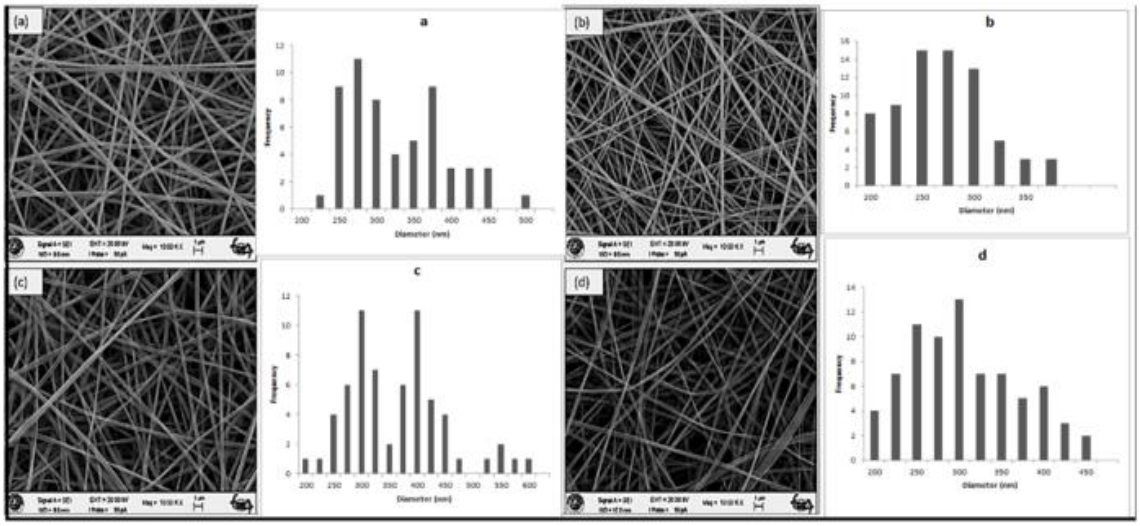

Figure 3. (a) Variation of dynamic viscosity of the solutions in function of copper nanoparticles contents (pure PAN 1, 3 and % 5 wt of CuNPs), (b) variation of average diameters against dynamic viscosity (mPa.s) of the solutions (c) variations of EC of nanofibers against dynamic viscosity (mPa.s) of the solutions. In (a) and (b) from left bar to right bar : pure PAN 1, 3 and 5 wt % of CuNPs, respectively

The dispersion of small amount (1 wt. %) of copper nanoparticles in the solution not only has led to a decrease of the average diameter of the as-spun nanofibers but also to the highest value of EC. The variation of EC of PAN fibers containing copper nanoparticles was summarized in the Table 1. In order to have an idea of the range of our results, in the Table 1, different results of this study were compared to the literature ones. To the best of our knowledge, the investigation of EC of PAN nanofiber containing copper has not yet been examined before. XRD was performed to give detailed information on the structure of crystalline samples and to confirm the phase composition of the as-spun nanofibers. According to the literatures, two peaks appear around $2\theta = 17°$ and $2\theta = 29°$ for the pure PAN. The peak associated with (100) plane of a orthorhombic semi-crystalline PAN structure appeared at $2\theta = 17°$ for pure PAN fibers [30, 31].

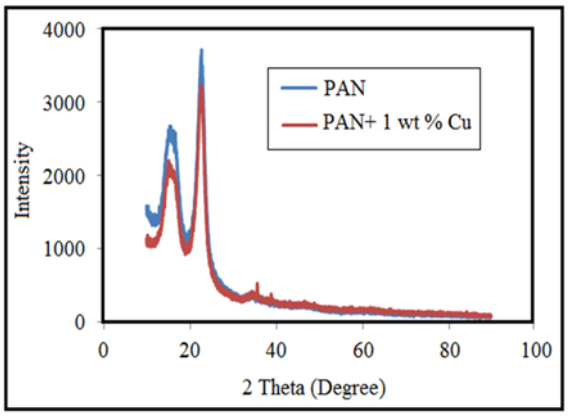

Figure 4. XRD patterns of pure PAN and PAN/CuNPs

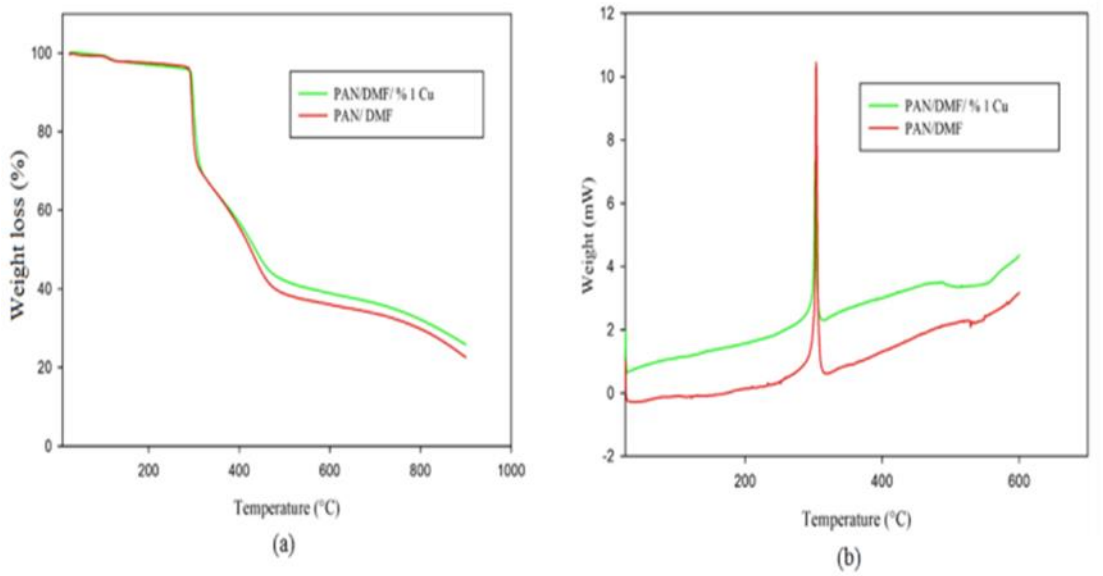

Figure 5. (a) TGA (b) DSC pattrens of pure PAN and PAN/CuNPs nanofibers

As can be seen in Figure 4, two peaks were found for either nanofibers sample. The first broad peak is located at around $2\theta = 16°$, which represents the x-ray reflection of the (100) plane in PAN [32] and reveals the amorphous state of materials. The second peak which was sharper than the first one was found at around $2\theta = 23°$ and reveals the crystalline structure of the materials. Furthermore, such peaks do not make any significant shifts but it was observed a decrease of the relative intensity of peaks when Cu nanoparticles were added in the electrospinning solution [33]. Although two small peaks were found at around $2\theta = 36°$ and $2\theta = 39°$ for samples containing copper nanoparticles, it can hardly be attributed to copper nanoparticles due to the fact that a closer inspection revealed that the positions of these peaks are different to those of pure copper nanoparticles. The decrease in the PAN peak intensity indicates that CuNPs were successfully incorporated and homogeneously dispersed in the material matrix [34].

Thermogravimetric analyzer (TGA) and differential scanning calorimetry were employed in order to study the thermal behavior of the as-spun nanofibers. Figure 5a and Figure 5b show the TGA-DTA and DSC patterns of pure PAN and PAN/CuNPs nanofibers, respectively. The investigation revealed that there are striking similarities between pure PAN and PAN/Cu nanofibers decomposition process. The TGA thermograms of pure PAN nanofibers showed % 77.2 of weight loss for samples obtained from 15 kV as electrospinning voltage. And their respective amount of waste materials were % 22.8 by mass after reaching 900 °C. PAN-doped PAN nanofiber shows a mass loss of 75 % up to 900 °C. The amount of waste at 900 ºC was determined as 25%. As can be seen in Table 2, weight loss values of PAN/Cu fibers were less than those of pure PAN fibers. Therefore, inorganic residuals values were higher than those of pure PAN fibers after reaching 900 °C. What is more, comparing the onset temperatures of the resultant nanofibers a slight enhancement of the thermal stability was observed with the addition of 1wt % of copper nanoparticles. These results confirm the existence of nanoparticles in the as-spun nanofibers.

Calculation of the composite fiber content can be done by three different methods. This calculation can be done according to the titration method, optical microscopy related techniques, resin burning method and TGA analysis. After the formation of PAN fibers, the amount of nanoparticle in the fiber content and the amount of matrix PAN were calculated from TGA. TGA thermograms of weight loss as a function of temperature at 100-450 ºC for the neat PAN [35].

The component content of the as-spun composite fibers was calculated according to the Equation 1 [31] and the weight content data were presented in Table 2.

$$\text{PAN content } \% = \frac{\text{Composit fiber } \% \text{ decomposition} - \text{Cu } \% \text{ decomposition}}{\text{PAN pure } \% \text{ decomposition } - \text{Cu } \% \text{ decomposition}} \quad (1)$$

The glass translation temperatures of pure PAN fiber was 112 °C. An endothermic peak of the glass transition temperature was not observed in the 1 wt. % copper-doped PAN nanofiber. Meanwhile, the DSC thermogram revealed that the crystallization peak temperatures of composite fibers and fiber containing 1wt % Cu were observed at 300 °C and 305 °C for fibers obtained from 15 kV, respectively. In addition, the melting point temperature of composite fibers was found to be 560 °C. Melting point increased by 20 °C with the addition of copper. The DSC related data are presented in Table 3.

EDX analysis images of PAN nanofibers with 1 wt %, 3 wt %, 5 wt % Cu nanoparticles are presented in Figure 6a, b, c. TEM images of Cu/PAN nanofibers are shown in Figure 6d-e. The presence of copper nanoparticles from the existing atomic contents of nanofibers has been proven.

Surfaces providing water contact angle lower than 90° are considered as hydrophilic. However, when contact angles higher than 90°, surfaces are regarded as hydrophobic and surfaces presenting a contact angle higher than 150° are designed as super-hydrophobic [36-39].

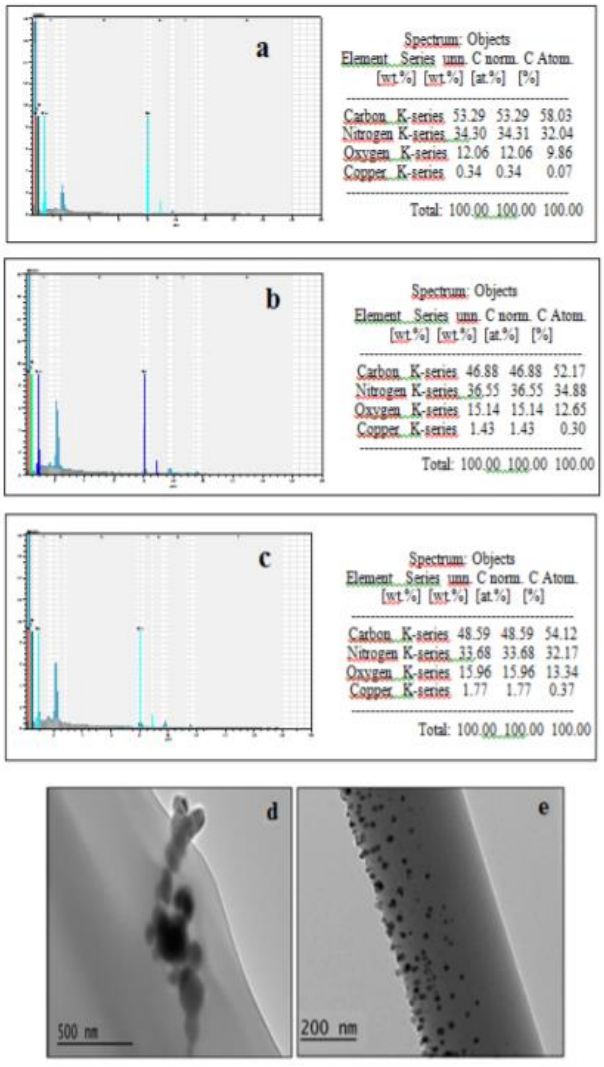

Figure 6. EDX and TEM images of Cu/PAN nanofibers
(a) PAN nanofibers with 1 wt % CuNPs (b) PAN nanofibers with 3 wt % CuNPs (c) PAN nanofibers with 5 wt % CuNPs
d-e) TEM images of Cu/PAN nanofiber

In this study, only nanofibers samples which presented the highest values of EC were picked out for hydrophobicity investigation. Therefore, the static contact angles of fibers containing 1 wt. % of copper nanoparticles were investigated.

Table 1. Comparison of EC values for nanofibers/nanofibers with nano particules [40]

Chemicals	Electrical conductivity (S/cm)	References	Comments
Pure PAN in DMF	$5.81E^{-03}$	This study	Nanofibers produced at 15 kV
PAN/DMF/ Cu	$1.38E^{-02}$	This study	Nanofibers produced at 15 kV
Pure PAN in DMF	0.2 – 0.5	[20]	EC of the pure PAN nanofiber changed with the carbonization temperature
Pure PAN in DMF	$6.8\ E^{-03}$ and 1.96	[21]	Carbonized at 700 and 1000°C, respectively
Pure PAN in DMF	1.42	[22]	Carbonized at 1000°C
Nylon-6 with polyaniline	1.3	[23]	Polymerization technique. Randomly oriented nanofiber membrane fiber
Polypyrrole [PPy(SO_3H)-DEHS]	$2.7\ E^{-02}$	[24]	Not blending. Randomly oriented nanofiber membrane fiber.
Poly(L-lactide) with polyaniline	0.3	[25]	Randomly oriented nanofiber membrane fiber
Polyvinyl alcohol with Nafion (1:5)	$1.7\ E^{-02}$	[26]	Randomly oriented nanofiber membrane fiber
Poly(methyl methacrylate) with 2 wt. % multi-walled carbon nanotube	$5.3\ E^{-04}$	[27]	Blending technique. Single fiber
Silk membrane coated with multi-walled carbon nanotube	$2.4\ E^{-04}$	[28]	Surface coating by dipping in carbon nanotube suspension.Randomly oriented nanofiber membrane fiber
Polyethylene oxide with polypyrrole coating	$1\ E^{-03}$	[29]	Surface polymerization. Randomly oriented nanofiber membrane fiber
PAN/DMF/ SiO_2	$8.26E^{-03}$	[41]	Nanofibers produced at 15 kV

The contact angle measurement results revealed that nanofibers containing 1 wt. % of copper nanoparticles showed a hydrophobic behavior. As illustrated in Figure 7, there was a slight difference between both contact angle values of composite nanofibers. It is important to note how the hydrophobic behavior of nanofibers (pure PAN and PAN/ 1 wt. % Cu fibers) surfaces was improved in both cases by adding 1 wt. %, from 120.18° to 124.93°. To the light of these results, the surfaces of the as-spun fibers were found to be hydrophobic. It is thought that the increase in surface contact angle of copper doped and PAN fibers is due to the increase of roughness on the fiber surface.

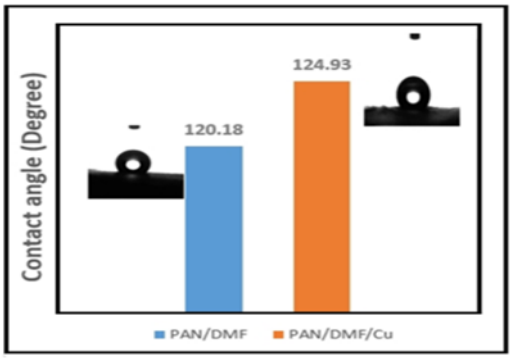

Figure 7. Average static contact angles of the as-fabricated pure PAN and PAN/Cu fibers

Table 2.TGA data and weight content (%) of pure PAN and PAN/Cu composite fibers

Fibers	IDT (ºC)	Max.T_d (ºC)	T_5 (ºC)	$T_{9\ or}\ T_{10}$ (ºC)	Residual weight at 900 °C (%)	Fibers Weight content (%)	
						Cu %	PAN %
Pure PAN 150000 g/mol (15 kV)	290	295	293	298	23	-	100
15kV PAN/Cu (%1)	290	300	265	310 T_{10}	25	1.8	98.2

Max.T_d - maximum decomposition temperature, IDT- Initial decomposition temperature, T_5 - 5% weight decomposition, $T_{9\ or}\ T_{10}$- 10% weight decomposition

Table 3. DSC data of PAN/Cu composite fibers for 15 kV

Composite fibers	Tg (°C) (Tg *= (104.9 °C)	Tc $_{(exo)}$ (°C)	Tm $_{(endo)}$ (°C)
PAN	112	301	540
PAN/Cu (%1)	-	300	560

4 Conclusion

In this study, pure PAN fibers and composite nanofibers containing 1, 3 and 5 wt. % of copper contents were successfully prepared by using electrospinning technique. The effect of copper nanoparticles on the morphology and diameters of composite fibers was investigated. It was found that fibers with smaller diameters were obtained with the decrease of copper contents in the solution. In addition, both pure PAN nanofibers and composite fibers were beads-free, uniform and without agglomeration of copper nanoparticles on the surface of the as-spun nanofibers. The EC of the as-spun fibers was investigated in terms of the copper contents. With the addition of % 1 wt. of copper nanoparticles, the EC of the obtained fibers increased, however, it was observed that as the copper content increased the EC decreased. In this study, the highest conductivity was obtained with %1 wt. Cu/PAN fibers obtained by electrospinning solution having a dynamic viscosity value of 577.7 mPa.s. The contact angle results revealed that the addition of 1wt % of copper nanoparticles enhanced slightly the hydrophobic behavior of the composite fibers.

Acknowledgements

Authors acknowledged a financial support received from the research fund of the Selcuk University under Grant No. BAP 17201017.

References

[1] Wang, C., Du, J., Wang, S., Li, Y., Chen, X., Jing, X., Wei, Y., Preparation of silver nanoparticles dispersed in polyacrylonitrile nanofiber film spun by electrospinning, *Materials Letters* 59, 3046-3049, 2005.

[2] Mazinani, S., Ajji, A., Dubois, C., Morphology, structure and properties of conductive PS/CNT nanocomposite electrospun mat, *Polymer*, 50: 3329-3342, 2009.

[3] Sichani, G.N., Morshed, M., Amirnasr, M., Abedi, D., In situ preparation, electrospinning, and characterization of polyacrylonitrile nanofibers containing silver nanoparticles, *Journal of Applied Polymer Science*, 116, 1021-1029, 2010.

[4] Jeong, L., Park, W.H., Preparation and characterization of gelatin nanofibers containing silver nanoparticles, *International Journal of Molecular Sciences*, 15, 6857-6879, 2014.

[5] Huang, Z.M., Zhang, Y.Z., Kotaki, M., Ramakrishna, S., A review on polymer nanofibers by electrospinning and their applications in nanocomposites, *Composites Science and Technology*, 63, 2223-2253, 2003.

[6] Li, D., Xia, Y., Electrospinning of nanofibers: reinventing the wheel?, *Advanced Materials*, 16, 1151-1170, 2004.

[7] Shi, X., Zhou, W., Ma, D., Ma, Q., Bridges D., Ma, Y., Hu, A., Electrospinning of nanofibers and their applications for energy devices, *Journal of Nanomaterials*, Volume 2015, 20 pages, 2015.

[8] Ding, B., Yu, J., Electrospun nanofibers for energy and environmental applications, Springer, 2014.

[9] Ramakrishna, S., An introduction to electrospinning and nanofibers, World Scientific, 2005.

[10] Frenot A., Chronakis, I.S., Polymer nanofibers assembled by electrospinning, *Current Opinion in Colloid & Interface Science*, 8, 64-75, 2003.[11] Karakaş, H., Electrospinning of Nanofibers and There Applications, Istanbul Technical University, Textile Technologies and Design Faculty, 2015.

[12] Fong, H., Chun, I, Reneker, D., Beaded nanofibers formed during electrospinning, *Polymer*, 40, 4585-4592, 1999.

[13] McKee, M.G., Wilkes, G.L., Colby, R.H., Long T.E., Correlations of solution rheology with electrospun fiber formation of linear and branched polyesters, *Macromolecules*, 37, 1760-1767, 2004.

[14] Tański, T., Matysiak, W, Hajduk, B., Manufacturing and investigation of physical properties of polyacrylonitrile nanofibre composites with SiO_2, TiO_2 and Bi_2O_3 nanoparticles, *Beilstein Journal of Nanotechnology*, 7, 1141-1155, 2016.

[15] Rujitanaroj, Po., Pimpha, N., Supaphol, P., Preparation, characterization, and antibacterial properties of electrospun polyacrylonitrile fibrous membranes containing silver nanoparticles, *Journal of Applied Polymer Science*, 116, 1967-1976, 2010.

[16] Luoh, R., Hahn, H.T., Electrospun nanocomposite fiber mats as gas sensors, *Composites Science and Technology*, 66, 2436-2441, 2006.

[17] Deng, C., Gong, P., He, Q., Cheng, J., He, C., Shi, L., Zhu D., Lin T., Highly fluorescent TPA-PBPV nanofibers with amplified sensory response to TNT, *Chemical Physics Letters*, 483, 219-223. 2009.

[18] Wang, X., Lin, T., Needleless electrospinning of nanofibers: Technology and applications, CRC Press, 2013.

[19] Lee, D.Y., Kim, B.Y., Lee, S.J., Lee M.H., Song Y.S., Lee, J.Y., Titania nanofibers prepared by electrospinning, *Korean Physical Society*, 48 (6), 1686-1690, 2006.

[20] Ra, E.J., An, K.H., Kim, K.K., Jeong, S.Y., Lee, Y.H., Anisotropic electrical conductivity of MWCNT/PAN nanofiber paper, *Chemical Physics Letters*, 413, 188-193, 2005.

[21] Kim, C., Kim, J.S., Lee, W.J., Kim, H.S., Edie, D.D., Yang, K. S., Preparations of PAN-based Activated Carbon Nanofiber Web Electrode by Electrostatic Spinning and Their Applications to EDLC, *Journal of the Korean Electrochemical Society*, 5, 117-124, 2002.

[22] Panapoy, M, Dankeaw A., Ksapabutr, B., Electrical conductivity of PAN-based carbon nanofibers prepared by electrospinning method, *Thammasat Int. J. Sc. Tech*., 13, 11-17, 2008.

[23] Hong, K.H., Oh, K.W., Kang, T.J., Preparation of conducting nylon-6 electrospun fiber webs by the in situ polymerization of polyaniline, *Journal of Applied Polymer Science*, 96, 983-991, 2005.

[24] Chronakis, I.S., Grapenson, S., Jakob., A., Conductive polypyrrole nanofibers via electrospinning: electrical and morphological properties, *Polymer*, 47, 1597-1603, 2006.

[25] Dong, H., Prasad, S., Nyame, V., Jones, W.E., Sub-micrometer conducting polyaniline tubes prepared from polymer fiber templates, *Chemistry of Materials*, 16, 371-373, 2004.

[26] Laforgue, A., Robitaille, L., Mokrini, A., Ajji, A., Fabrication and characterization of ionic conducting nanofibers, *Macromolecular Materials and Engineering*, 292, 1229-1236, 2007.

[27] Sundaray, B., Choi, A., Park, Y.W., Highly conducting electrospun polyaniline-polyethylene oxide nanofibrous membranes filled with single-walled carbon nanotubes, *Synthetic Metals*, 160, 984-988, 2010.

[28] Kang, S.J., Kocabas, C., Ozel, T., Shim, M., Pimparkar, N., Alam, M. A., Rotkin, S.V., RogersJ. A., High-performance electronics using dense, perfectly aligned arrays of single-

walled carbon nanotubes, *Nature Nanotechnology*, 2, 230-236, 2007.

[29] Nair, S., Natarajan, S., Kim, S.H., Fabrication of electrically conducting polypyrrole-poly (ethylene oxide) composite nanofibers, *Macromolecular Rapid Communications*, 26, 1599-1603, 2005.

[30] Chhatbar, M.U., Meena, R., Prasad, K., Siddhanta, A.K., Agar/sodium alginate-graft-polyacrylonitrile, a stable hydrogel system, *Indian Journal of Chemistry*, 48A, 1085-1090, 2009.

[31] Rajendran, S., Kannan, R, Mahendran, O., Study on Li ion conduction behaviour of the plasticized polymer electrolytes based on polyacrylonitrile, *Materials Letters*, 48: 331-335, 2001.

[32] Zussman, E., Chen, X., Ding, W., Calabri, L., Dikin, D.A., Quintana J.P., Ruoff, R.S., Mechanical and structural characterization of electrospun PAN-derived carbon nanofibers, *Carbon*, 43, 2175-2185, 2005.

[33] Robinson, J.W., Frame, E.S, Frame II, G.M., Undergraduate instrumental analysis, CRC press, 2014.

[34] Mohamed, S.A., Al-Ghamdi, A., Sharma, G., El Mansy, M.K., *Journal of Advanced Research*, 5, 79-86, 2014.

[35]Khan, W.S, Ceylan, M., Jabarrania, A., Saeednia, L., Asmatulu, R., Chemical and thermal ınvestigations of electrospun polyacrylonitrile nanofibers incorporated with various nanoscale inclusions, *Journal of Thermal Engineering*, 3, 1374-1389, 2017.

[36] Lafuma, A., Quéré, D., Superhydrophobic states, *Nature* Materials, 2, 457-460, 2003.

[37] Yuan, Y., Lee, T.R., Contact angle and wetting properties, Surface Science Techniques, Springer, 3-34, 2013.

[38] Liu, Y., Chen, X., Xin, J., Super-hydrophobic surfaces from a simple coating method: a bionic nanoengineering approach, *Nanotechnology*, 17 (13), 3259-3263, 2006.

[39] Gao, L., McCarthy, T.J., A perfectly hydrophobic surface (θA/θR= 180/180), *Journal of the American Chemical Society*, 128, 9052-9053, 2006.

[40] Mpukuta, O.M., Investigation of electricalconductivity of nanofibers (PAN) containing nanoparticles (graphene, copper,silica) produced by electrospinning method,Selcuk University Graduate School of Natural And Applied Sciences, *Master of Science Thesis*, Department of Mechanical Engineering M.Sc.

[41] Mpukuta, O.M., Dincer, K., Erdal, M.O., Investigation of electrical conductivity of PAN nanofibers containing silica nanoparticles produced by electrospinning method, *Materials Today: Proceedings*, 18 (5), 1927-1935, 2019.

International Journal of Innovative Engineering Applications

Journal homepage: https://dergipark.org.tr/ijiea

INFESTATION RATE OF ALMOND SEED WASP (*EURYTOMA AMYGDALI* ENDERLEIN, HYMENOPTERA: EURYTOMIDAE) ON IMPORTANT COMMERCIAL ALMOND VARIETIES IN MALATYA PROVINCE (TURKEY)

Talip Yiğit*[1], İnanç Özgen[2], Adnan Canbay[1], İbrahim Koç[3]

[1]*Apricot Research Institute, Malatya, Turkey*

[2]*Fırat University, Faculty of Engineering, Department of Bioengineering, Turkey*

[3]*Bitlis Eren University, Faculty of Engineering and Architecture, Department of Environmental Engineering, Turkey*

Abstract

Original scientific paper

Almond seed wasp (*Eurytoma amygdali* Enderlein) (Hymenoptera: Eurytomidae) is one of the most important pests of almond. Pest's infestation ratio can be as high as 95% in some areas in case if the pest is not tackled. The study was conducted to determine the preferences of Almond seed wasp seed wasp for some almond varieties (Ferragnes, Ferraduel, Nonpareil, Drake, Cristomorto and Garrigues) in the years 2017 and 2018. Furthermore, times of emerging of the pest in Malatya Province and the number of individuals emerging from damages fruits based on years were determined. Cage observations were carried out and fruits were counted under field conditions and results were discussed with meteorological data. As a result of the study, it was found that the lowest infestation rate of *E. amygdali* was in Ferragnes variety (81%) followed by Cristomorto variety (85%) while the highest infestation rate was found in Nonpareil variety (97%). While the rate of emerging of the pests as adults in 2017 was 89.3%, rate of individuals passing down to the next generation was 10.6%. It was found in the study that the time of emergence as adults of Almond seed wasp seed wasp in Malatya was the end of April when the maximum air temperature was 25ºC and the daily mean temperature is higher than 15ºC, and when the temperatures are routinely around these levels.

Keywords: *Almond, Eurytoma amygdali, Infestation rate, IPM*

1 Introduction

Global almond production is about 2.25 million tons. USA takes the first place with about 1 million tons. Turkey, however, takes the 5th place in the world with an annual production of 100,000 tons on an area of 42200 ha (TÜIK 2018; FAO 2017). There are several pest species that have adverse on this production amount. Almond seed wasp (*Eurytoma amygdali*) in almond cultivation lands is in the position of the most important species as regards the wideness of spread and loss ratio. It affects the product amount directly by creating damage on the fruit. It reproduces once a year or every two years (Anonymous, 2019). Almond seed wasp infestation rate occurs between 50% and 95% if there is no pest management applications (Cakar, 1980; Katsoyannos et al., 1992; Haltrich and Marko, 1998; Bolu and Özgen, 2007; Duval and Millan, 2010; Yeşilyaprak, 2015). There are many studies on the biology, natural enemies, form of damage caused by and control of the pest. However, studies carried out with the purpose of determining the preference of the pest among the almond varieties are limited in number. the control strategies of almond seed wasp is generally based on determining the time of emerging of the adults, and keeping the trees treated with pesticides throughout the emerging period of adults in order to destroy them before mating and laying eggs (Anonymous, 2019). However, chemicals have adverse effects on humans, environment, balance of the nature and they also can increase tolerance of insects to the chemical. A way to reduce these adverse effects is the use of a variety resistant against the pest. It is possible to use less amounts of pesticides by using resistant varieties.

This study was conducted determine the preferences of *Eurytoma amygdali* for some almond varieties in Malatya province in years 2017 and 2018.

2 Material and Method

In this study, different almond varieties grown on the altitude of 1005 m in the almond application parcel of the Malatya Apricot Research Institute, Central Campus. *Eurytoma amygdali* Enderlein pest species, culture cages, chiffon branch cages and laboratory materials were used as main materials.

No chemical pesticides were used on the almond trees grown in the application parcel starting from the emerging time of almond seed wasp in the year 2017 till their period of laying eggs.

2.1 Determining the Time of Emerging of *Eurytoma amygdali*

One chiffon branch cage was installed on 3 almond trees in the application parcel on branches 1.5m in height

∗ Corresponding author.

E-mail address: talipyigit79@hotmail.com (T. Yiğit) | ORCID Number : 0000-0002-4871-9132

Received 15 May 2020; Received in revised form 12 June 2020; Accepted 13 June 2020

 Doi: https://doi.org/10.46460/ijiea.737755

before the blossoming of the tree (April 1). After following the phonologic period of the tree, and Then 10 fruits of the previous year infested with almond seed wasp were placed in each cage. Cages were checked weekly till the blossoming time and daily after blossoming in order to determine the first emerging adults of the pest. This process was evaluated together with the meteorological data obtained from the meteorology station.

2.2 Determining the Preference of the Pest among the Almond Varieties

The study was carried out on Ferragnes, Ferraduel, Nonpareil, Drake, Cristomorto and Garrigues almond varieties grown in the application parcel. This study was conducted to four repeatly rows of trees (four ages). No chemicals were applied on the trees starting from the end of the blossoming time. When the fruits reached the harvesting stage, 200 fruits in total for each variety each 50 belongs to each repeat row were harvested from the trees. All the fruits were picked on branches selected randomly from the same side and same height of each tree. Fruits harvested were brought in the laboratory and cracked in order to detect the pest. All the fruits were counted and subjected to Chi-Square test and percentage analyses to determine statistical differences between the varieties.

3 Results and Discussion

3.1 Determining the Emerging Time of *Eurytoma amygdali*

The initial emerging of adults from fruits infested with almond seed wasp in cages occurred in April 28, 2017. It was observed at that time that almond trees of the parcel was in the beginning stage of the phenological small fruit stage. Meteorological data obtained from Meteorology Station are given in Table 1.

Evaluation of the initial emerging time of the pest together with the meteorological data revealed that the initial emerging time of the pest started with the daily maximum temperature reached 25ºC and daily mean temperature reached 15ºC and when these temperatures became the routine. Yeşilyaprak (2015) has reported in a study that the initial emerging of the pest started on the second week of April, and the infestation rate reached 54% in Bozova District and 70% in the Central District in case no efforts are exerted to control the pest. Çağlar (2018), however, found that the date of initial emerging of the pest in Adıyaman Province, Kahta and Besni districts was 24-27 March, and the pest needed 207.1 – 228.2 day-degrees for emerging of adults in these districts.

Table 1. Temperature values of April, 2017.

Days	Daily maximum temperature (°C)	Daily minimum temperature (°C)	Daily average temperature (°C)
1	13,5	5,1	9,4
2	17,3	3,6	9,5
3	15,9	2,8	9,2
4	19,2	2,2	11,4
5	21,1	3,9	12,3
6	18,7	5,0	12,1
7	14,4	8,3	11,1
8	16,3	5,2	9,8
9	10,9	1,8	6,2
10	12,3	1,5	6,5
11	14,9	1,0	8,0
12	14,1	0,1	7,7
13	11,4	6,7	8,6
14	16,8	8,3	11,7
15	16,0	9,0	11,6
16	20,2	4,9	12,2
17	19,4	6,8	13,9
18	15,1	8,2	11,6
19	18,9	5,6	11,9
20	20,6	6,0	14,2
21	20,6	7,5	15,4
22	26,5	11,9	19,7
23	23,2	11,8	19,9
24	17,4	3,4	10,0
25	17,6	3,6	10,2
26	20,8	1,6	11,2
27	23,3	4,1	14,0
28	26,4	7,0	16,3
29	25,7	7,8	16,9
30	26,2	7,8	17,0

In their study on this pest carried out in France, Duval and Millan (2010) reported that the time of initial emerging of the pest was April 13 in 2005, April 18 in 2006 and April 2 in 2007. They also reported that a single pest control sufficed carried out at the beginning of the emerging of adults, ratio of infected fruits was as low as 1-4%, and the loss ratio in the control parcel that pest control was not carried out exceeded 60%. Ekici and Günaydın (1969) reported in their study conducted in Elazığ Province that *E. amygdali* caused product loss of 51% in almond cultivation areas in 1964. Bolu and Özgen (2007) reported that the almond orchards in Diyarbakır, Elazığ and Mardin provinces were infested with *E. amygdali* and infestation rate exceeded 50% in some cultivation lands.

3.2 Determining the Preference of *Eurytoma amygdali* among Almond Varieties

Data obtained in the study are given Table 2. Nonpareil variety was the most preferred by *E. amygdali* with %97 infestation rate while Ferragnes variety was the least preferred by almond seed wasp with 81%. Upon statistical evaluation of the preference of the pest among the almond varieties, differences are observed. However, although the Ferragnes variety was the least preferred one, its contamination rate is high resulting in serious loss of yield. In a study conducted in Kahramanmaraş within the years 2005 and 2006, Gökalp Barut (2007) reported that the highest contamination rate among 27 varieties and types was seen in Sonora almond variety with 84% and 88%. Infestation rate was reported between 1% and 88% although it different among varieties.

Results obtained in works carried out to determine the number of individuals of *E. amygdali* in years one and two are given in Table 3. Accordingly, the rate of emerging as adults of the pest in the year one was 89.3%, while the rate of individuals giving rise to the next generation was 10.6%.

In conclusion, consideration of all these data shows that the pest has some preference among the almond varieties to be certain level. However, this selectivity was not sufficient to reduce the level of loss under the economic loss level even in the least preferred variety. With this reason, the time for control of the pest must be determined and management applications must be initiated in areas where the pest is found in high populations disregarding the variety. Furthermore, studies involving the chemical control against the pest and use of varieties against the pest should be carried out together. This approach can emerge as a potential method that could reduce the population density.

Table 2. Loss Rate of *Eurytoma amygdali* on Important Commercial Varieties

Types	Fruit checked (pieces)	Fruit contaminated with pests (pieces) *	Pest contamination rate (%)
Ferragnes	200	162	81
Ferraduel	200	190	95
Nonpareil	200	194	97
Drake	200	182	91
Cristomorto	200	170	85
Garrigues	200	186	93

Table 3. Adult Outputs of *Eurytoma amygdali* by Years (pieces)

Total number of contaminated fruit checked	Number of adults emerging in 2017 (1^{st} year)	Number of adults emerging in 2018 (2^{nd} year)
178	159	19

References

Anonymous, 2019. T.C Tarım ve Orman Bakanlığı, Bitki Zararlıları Zirai Mücadele Teknik Talimatları.https://www.tarimorman.gov.tr/TAGEM/Belgeler/Bitki%20Zararl%C4%B1lar%C4%B1%20Zirai%20M%C3%BCcadele%20Teknik%20Talimatlar%C4%B1.pdf. Erişim tarihi: 06.01.2020.

Bolu, H. and Özgen, İ., (2007). Badem İçkurdunun (Eurytoma amygdali Enderlein) (Hymenoptera: Eurytomidae) Yayılış Alanları, Bulaşma Oranları ve Parazitoidleri. HR. Ü. Z.F. Dergisi, 11, (3/4) : (59-65).

Cakar, L. (1980). Eurytoma amygdali End.-(Hymenoptera, Chalcidoidea, Eurytomidae)-a pest of almond in Macedonia. Zastita Bilja, 31(3), 263-272.

Çağlar, Ö., (2019). Adıyaman İli Ticari Badem Bahçelerinde Badem İçkurdu, Eurytoma amygdali End. (Hymenoptera: Eurytomidae)'na Karşı En Uygun İlaçlama Zamanının Belirlenmesi. Yüksek lisans tezi (Basılmamış) Kahramanmaraş, s. 46.

Duval, H., and Millan, M. (2010). Emergence dates of Eurytoma amygdali Enderlein adults in the south-east of France and control strategy. In Options Mediterraneennes. Series A. Mediterranean Seminars (No. 94, pp. 175-180).

Ekici, V., and Günaydın, T. (1969). Investigation on Eurytoma amygdali End. in East and Southeast Anatolia. Bitki Koruma Bülteni Ek Yayın:1, s.28.

FAO,2017. http://www.fao.org/faostat/en/#data/QC. Erişim tarihi: 06.01.2020.

Gökalp Barut, G. B., (2007). Kahramanmaraş Koşullarında Bademlerde Zararlı Badem İç Kurdu, Eurytoma amygdali Enderlein (Hymenoptera: Eurytomıdae)'nin Bazı Biyolojik Özelliklerinin Belirlenmesi Üzerine Çalışmalar. Yüksek lisans tezi (Basılmamış) Kahramanmaraş, s. 33.

Haltrich, A., and Marko, V. (1998). Damage of almond seed wasp, Eurytoma amygdali Enderlein (Eurytomidae,

Hymenoptera) near Budapest. Novenyvedelem (Hungary) Vol.34 No.10 pp.545-549.

Katsoyannos, B. I., Kouloussis, N. A., and Bassiliou, A. (1992). Monitoring populations of the almond seed wasp, Eurytoma amygdali, with sex pheromone traps and other means, and optimal timing of chemical control. Entomologia experimentalis et applicata, 62(1), 9-16.

TÜİK, (2018). https://biruni.tuik.gov.tr/medas/?kn=92&locale=tr. Erişim tarihi: 06.01.2020

Yeşilyaprak, M., (2015). Şanlıurfa İli Badem Bahçelerinde Zararlı Olan Badem İçkurdu [(Eurytoma amygdali Enderlein, (Hymenoptera: Eurytomidae)]' nun Yaygınlığı Ve Zarar Durumunun Tespiti. Yüksek lisans tezi (Basılmamış) Şanlıurfa, s. 36.

International Journal of Innovative Engineering Applications

Journal homepage: https://dergipark.org.tr/ijiea

INVESTIGATION OF THE MECHANICAL BEHAVIOR OF RING SECTIONED TRANSMISSION STEELS COMBINED WITH DIFFERENT ADHESIVES

Anıl İmak*[1], Aydın Turgut[1]

[1]*Bingol University, Faculty of Engineering and Architecture, Department of Mechanical Engineering, Turkey*

Abstract

Original scientific paper

The aim of this study is to investigate the effect of the environmental adhesion surface on the bond strength of the ring-sectioned transmission steel bars on the butt. Male and female molds were produced in order to make the joints of the shafts. With two different adhesives (DP 410, DP 490), four different overlap distances (10mm, 20mm, 30mm, 40mm) and two different overlap angles (30º, 90º) rods are combined with the adhesive. Mechanical behavior of peripheral bonding surface of which is adhered with an overlap butt sample was assayed according to the determined parameters. Tensile and torsion experiments of ring cross-section rods combined with adhesive were performed. The graphs of the experimental data obtained were prepared and compared. DP 410 affixed with adhesive ring sectioned rod showed the better performance of the rods, prepared by the DP 490 adhesive.

Keywords: *Torsion, Stress analysis, Ring section bar, Adhesive*

FARKLI YAPIŞTIRICILARLA BİRLEŞTİRİLEN HALKA KESİTLİ TRANSMİSYON ÇELİKLERİNİN MEKANİK DAVRANIŞLARININ ARAŞTIRILMASI

Özet

Orijinal Bilimsel Makale

Bu çalışmanın amacı halka kesitli transmisyon çeliği çubukların alın alına bindirmeli olarak yapıştırılmasında çevresel yapışma yüzeyinin bağlantı mukavemetine etkisinin araştırılması amaçlanmıştır. Millerin alın alına birleştirmelerinin yapılabilmesi için erkek ve dişi kalıp olarak üretimleri yapılmıştır. İki faklı (DP410, DP490) yapıştırıcı ile dört farklı bindirme mesafesi (10mm, 20mm, 30mm, 40mm) ve iki farklı bindirme açısı (30º, 90º) çubuklar yapıştırıcı ile birleştirilmiştir. Belirlenen parametreler doğrultusunda alın alına bindirmeli olarak yapıştırılan numunelerin çevresel yapışma yüzeylerinin mekanik davranışları incelenmiştir. Yapıştırıcıyla birleştirilmiş halka kesitli çubukların çekme ve burulma deneyleri yapılmıştır. Elde edilen deneysel verilerin grafikleri hazırlanmış ve değerlendirilerek kıyaslanmıştır. DP410 yapıştırıcıyla yapıştırılmış halka kesitli çubuklar DP 490 yapıştırıcıyla hazırlanmış olan çubuklara göre daha iyi performans göstermiştir.

Anahtar kelimeler: *Burulma, gerilme analizi, Halka kesitli çubuk, Yapıştırıcı*

1 Giriş

Otomotiv endüstrisinde kullanılan güç iletim sistemlerinin en önemli elemanlarından biri olan miller (şaft), çalışma yapısı bakımından genellikle eğilme ve burulmaya maruz kalmaktadırlar. Günümüz endüstrisinde kompozit, plastik ve metal malzemelerin birleştirmelerinde kaynak, perçin lehim ve yapıştırıcı ile bağlantı yöntemleri kullanılmaktadır. Yapıştırıcı ile bağlantı oluşturma, yaygın bir kullanım alanı olan ve gün geçtikçe hızlı bir şekilde kullanımında artış gösterilen bir yöntemdir [1-2]. Yapıştırma yöntemi kullanılarak yapılan birleştirmenin, kaynak yöntemine göre yüksek sıcaklık ve lehimlemede gerekli olan metal malzeme ihtiyacını ortadan kaldırmaktadır [3]. Kaynak ile birleştirme yönteminde perçinlemedeki malzemenin birleştirme elemanı olan perçin birleştirme bölgesinden uzaklaştırması, korozyon ve kalıntı ısıl gerilimlerin oluşmasına sebep olmaktadır. Bu oluşum metal-metal birleşimlerinde ön yükleme gibi bağlantı dayanımlarını düşüren dezavantajlar oluşturmaktadır. Ayrıca geleneksel yöntemler ile birleştirmede ortamdaki nemden veya sıvı ile temasında metal-metal birleşimlerin teması kesilmediğinden dolayı korozyon artarak birleştirmenin dayanım süresini azaltmaktadır. Özellikle sulu ortamlardaki yoğun olarak basınçlı akışkan taşındığı düşünülen metal boruların kaynak yöntemi kullanılarak birleştirilmesinde zamanla korozyona sebep olmaktadır. Mikro boyuttaki bir çatlağın dahi basınçlı bir akışkan taşıyan bu boruda büyük hasar boyutları oluşturabilmektedir [4-5].

Metal-metal birleştirme bölgelerindeki iyileştirmelerde hassasiyetlere karşılık verebildiği için yapıştırıcı yöntemi, endüstriyel bir birleştirme yöntemi olarak tercih edilmeye başlamıştır. Yaygınlaşan yapıştırıcı kullanımı ile birlikte birleştirmede en önemli parametrelerin elde edilmesi içinde literatürde birçok araştırma ve geliştirme çalışmaları yapılmaktadır [6-9].

∗ Corresponding author.

E-mail address: aimak@bingol.edu.tr (A.İmak) | ORCID Number : 0000-0001-6091-1584

Received 11 February 2020; Received in revised form 7 March 2020; Accepted 9 March 2020

 Doi: https://doi.org/10.46460/ijiea.687503

Jeroen ve ark., yaptıkları çalışmada standart API hat borusu kuplajının yorulma davranışını deneysel olarak incelemişlerdir [10]. Kaplin geometrisinin yorulma ömrüne etkisini, 4 nokta eğilme yorulma testiyle incelemişlerdir. Elde ettikleri verileri deneysel ve sayısal olarak değerlendirmişlerdir. Vaziri ve ark., çalışmalarında harmonik bir eksenel yüke maruz kalan yapışkan olarak bağlanmış tübüler eklemlerin dinamik tepkilerini belirlemişlerdir [11]. Borulu eklem geometrilerinin, malzeme özelliklerinin ve yapışkan özelliklerinin sistemin dinamik tepkisi üzerine etkilerini incelemişlerdir. Das ve ark., yaptıkları çalışmada iç basınca maruz tabakalı FRP kompozit borular ile yapıştırılmış soket bağlantılarının üç boyutlu gerilme analizini yapmışlardır [12]. Li ve ark. çalışmalarında korozyon önleyici plastik alaşımlı kompozit boruya yapıştırılmış yapışkan metal parçasının gerilme analizini incelemişlerdir [13]. Rohem ve ark. Bu çalışmada borularda tamir için yeni bir polimerik matris kompozitin incelemesini yapmışlardır. İlk önce, mekanik ve termal olmak üzere yeni geliştirilen kompozit tabakanın özelliklerini belirlemişler ve borunun performansının değerlendirilmesini hidrostatik testlerle yapmışlardır [14]. Liu ve ark., çalışmalarında CFRP yamaları ile tamir edilmiş çatlağı olan alüminyum alaşımlı boru performanslarını tam olarak anlamak için 7005 tipi ticari borularda bir dizi yorulma ve yarı-statik testler yapmışlardır. Yapay çatlaklar ile hasar görmüş olan boru şekillendirilmiş CFRP yamaları ile sarılmıştır. Onarım işleminde vida dişi ve mekanik taşlama yöntemleri uygulanmıştır. Yama uzunluğunun ve katman sayısının etkileri aynı zamanda değerlendirilmiştir. Optimize olarak tasarlanmış CFRP yaması onarılmış alüminyum boruların yorulma testlerinde en iyi sonuçları vermiştir[15].

Yapılan literatür [1-15] incelemelerinde halka kesitli parçaların yapıştırıcı ile birleştirilmeleri neredeyse hiç çalışılmadığı görülmüştür. Bu sebeple bu çalışmada farklı özelliklere sahip iki tür yapıştırıcı ile birbirine geçmeli olarak birleştirilen halka kesitli transmisyon millerinin mekanik ve burulma davranışları araştırılmıştır.

2 Material ve yöntem

Deney çalışmalarında, Max. %0.2 C, %0.007 N, %0.05 P ve %0.05 S kimyasal kompozisyona sahip ve akma dayanımı 235 MPa, çekme dayanımı ise 360-460 MPa arasında olan St37 standartlarında, 30 mm çapında transmisyon çeliği ve DP410 ile DP490 yapıştırıcılar kullanıldı. Yapıştırıcılara ait özellikler ise Tablo 1 de verilmiştir. Birleştirme öncesi çubuklar torna tezgâhında Şekil 1' de verildiği gibi birbiri içine geçmeli olacak şekilde hazırlandı. Birleştirme işlemleri, Şekil 2' de gösterildiği gibi ve Tablo 2' de ki parametreler kullanılarak yapılmıştır. Standartlara uygun olarak hazırlanan DP 410 ve DP 490 bulk numuneleri ve yapıştırıcı ile birleştirilmiş numunelerin çekme deneyleri Batman Üniversitesi, Mühendislik Mimarlık Fakültesi Makine Mühendisliği Bölümü Laboratuvarı'nda bulunan SHMADZU marka ve 250000 N kapasiteye sahip çekme test cihazında yapılmıştır. Birbiri içine geçmeli olarak üretilen numuneler daha sonra DP410 ve DP490 yapıştırıcılarıyla birleştirilip burulma analizleri de yapılmıştır. Bu analizler Atatürk Üniversitesi Mühendislik Fakültesi Makine Mühendisliği Bölümü Laboratuvarı'nda JİNAN NDW-200 marka ve maksimum çalışma torku 170 N.m olan burulma cihazında gerçekleştirilmiştir

Tablo 1. DP 410 ve DP 490 yapıştırıcılarının özellikleri.

	DP410	DP490
Yapışkanın cinsi	Epoksi	Epoksi
Renk	Kirli Beyaz	Siyah
Viskozite	Tiksotroptik	Tiksotroptik
Soyma Dayanımı (Al, N/cm)	100	92
Kayma Dayanımı (Al - MPa)	34	30.2
Kürleşme Zamanı (dk)	25-30	200-240
Kuruma Zamanı (dk)	8-10	180

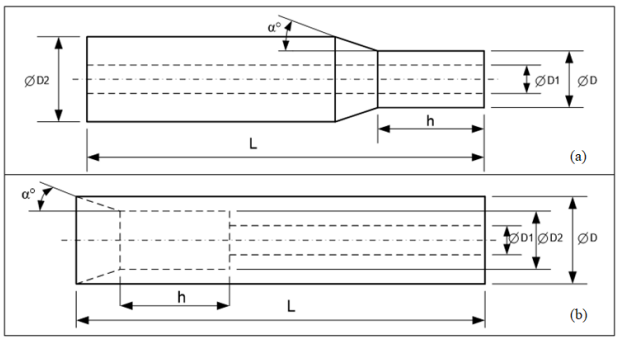

Şekil 1. Halka kesitli çubuk numunelerin parametreleri (a) erkek numune, (b) dişi numune

Şekil 2. Yapıştırıcıyla birleştirilmiş numune

Tablo 2. Çalışmada kullanılan numunelerin parametreleri

Numune No:	D (mm)	D1 (mm)	D2 (mm)	L (mm)	h (mm)	a° (derece)
1	30	10	15	100	10	30
2	30	10	20	100	10	30
3	30	10	15	100	20	30
4	30	10	20	100	20	30
5	30	10	15	100	30	30
6	30	10	20	100	30	30
7	30	10	15	100	40	30
8	30	10	20	100	40	30
9	30	10	15	100	10	90
10	30	10	20	100	10	90
11	30	10	15	100	20	90
12	30	10	20	100	20	90
13	30	10	15	100	30	90
14	30	10	20	100	30	90
15	30	10	15	100	40	90
16	30	10	20	100	40	90

Çalışmada kullanılan numunelerin çekme deneylerinde S harfi, burulma deneylerinde ise T harfi kullanılmıştır. Ayrıca DP410 ve DP490 yapıştırıcıları ise alt indis olarak belirtilmiştir. Örneğin, çekme deneyinde 1 nolu numunenin DP410 ile yapıştırılması durumunda $S1_{410}$ şeklinde, burulma için ise $T1_{410}$ olarak belirtilmiştir.

3 Sonuçlar ve tartışma

3.1 DP410 ile Birleştirilen Numunelerde 'h' Bindirme Mesafesinin Çekme Kuvvetine Etkisinin İncelenmesi

Yapıştırma işleminde DP410 kullanılan ve aynı bindirme çapı ile iç çapına sahip numunelerde 'h' değişiminin etkisine bakılmıştır. Dört farklı bindirme mesafesinin kıyaslanmasıyla oluşturulan grafikler Şekil 3, 4, 5 ve 6'da sırasıyla verilmiştir.

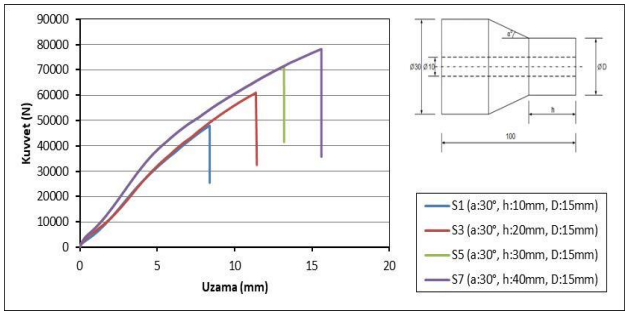

Şekil 3. DP410 yapıştırıcı kullanarak birleştirilen $S1_{410}$(a:30°, h:10mm, D:15mm), $S3_{410}$ (a:30°, h:20mm, D:15mm), $S5_{410}$ (a:30°, h:30mm, D:15mm) ve $S7_{410}$ (a:30°, h:40mm, D:15mm) nolu numunelerde 'h' bindirme mesafesinin çekme kuvvetine etkisi

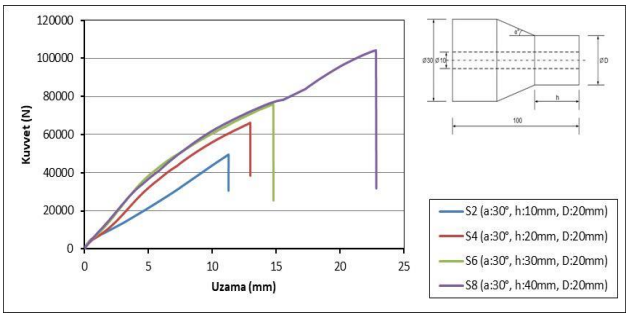

Şekil 4. DP410 yapıştırıcı kullanarak birleştirilen $S2_{410}$ (a:30°, h:10mm, D:20mm), $S4_{410}$ (a:30°, h:20mm, D:20mm), $S6_{410}$ (a:30°, h:30mm, D:20mm) ve $S8_{410}$ (a:30°, h:40mm, D:20mm) nolu numunelerde 'h' bindirme mesafesinin çekme kuvvetine etkisi

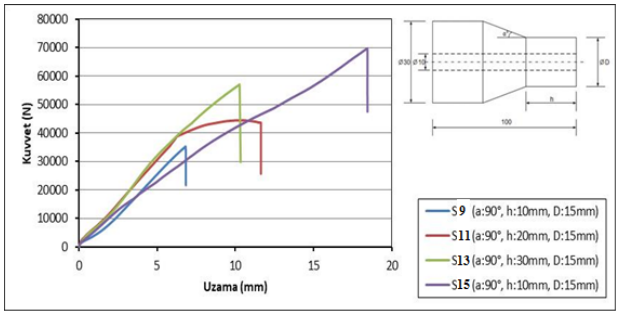

Şekil 5. DP 410 yapıştırıcı kullanarak birleştirilen $S9_{410}$ (a:90°, h:10mm, D:15mm), $S11_{410}$ (a:90°, h:20mm, D:15mm), $S13_{410}$ (a:90°, h:30mm, D:15mm) ve $S15_{410}$ (a:90°, h:40mm, D:15mm) nolu numunelerde 'h' bindirme mesafesinin çekme kuvvetine etkisi

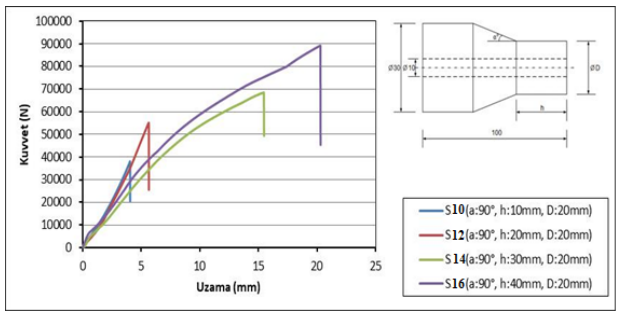

Şekil 6. DP410 yapıştırıcı kullanarak birleştirilen $S10_{410}$ (a:90°, h:10mm, D:20mm), $S12_{410}$ (a:90°, h:20mm, D:20mm), $S14_{410}$ (a:90°, h:30mm, D:20mm) ve $S16_{410}$ (a:90°, h:40mm, D:20mm) nolu numunelerde 'h' bindirme mesafesinin çekme kuvvetine etkisi

DP410 yapıştırıcısı kullanılarak dört farklı (10mm, 20mm, 30mm, 40mm) h bindirme mesafelerinde halka kesitli çubukların birleştirilmesi yapılmıştır. Yapılan birleştirmelerde h bindirme mesafesinin bağlantı mukavemetine etkisini incelemek için DP410 ile birleştirilmiş numuneler çekme yüküne maruz bırakılmıştır. Birleştirmelerin çekme kuvvetleri altındaki davranışları incelendiğinde genel olarak h bindirme mesafesi artıkça çekme yükünün arttığı görülmüştür. Çekme kuvvet değerleri incelendiği, maksimum ve minimum çekme kuvveti değerleri $S8_{410}$ ve $S9_{410}$ nolu numuneler de sırasıyla 104226.6 N ve 35328,13 N olarak elde edilmiştir. Bu durumun h bindirme mesafesinin artmasına paralel olarak yapışma yüzey alanın artmasına bağlı olduğu düşünülmektedir.

3.2 DP490 ile Birleştirilen Numunelerde 'h' Bindirme Mesafesinin Çekme Kuvvetine Etkisinin İncelenmesi

Yapıştırma işleminde DP490 kullanılan ve aynı bindirme çapı ile iç çapına sahip numunelerde 'h' değişiminin etkisine bakılmıştır. Dört farklı bindirme mesafesinin kıyaslanmasıyla oluşturulan Şekil 7, 8, 9 ve 10'da sırasıyla verilmiştir.

DP490 yapıştırıcısı kullanılarak dört farklı (10mm, 20mm, 30mm, 40mm) h bindirme mesafelerinde halka kesitli çubukların birleştirilmesi yapılmıştır. Yapılan birleştirmelerde h bindirme mesafesinin bağlantı mukavemetine etkisini incelemek için DP490 ile birleştirilmiş numuneler çekme yüküne maruz bırakılmıştır. Birleştirmelerin çekme kuvvetleri altındaki davranışları incelendiğinde genel olarak h bindirme mesafesi artıkça çekme yükünün arttığı görülmüştür.

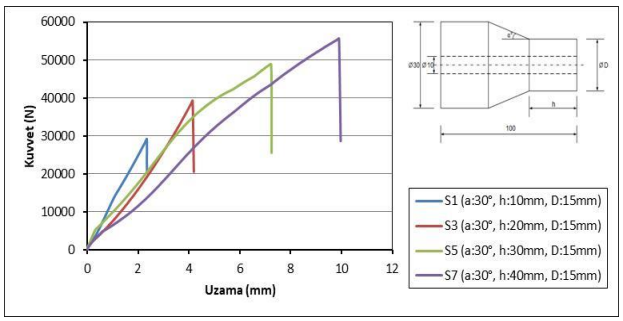

Şekil 7. DP 490 yapıştırıcı kullanarak birleştirilen $S1_{490}$ (a:30°, h:10mm, D:15mm), $S3_{490}$ (a:30°, h:20mm, D:15mm), $S5_{490}$ (a:30°, h:30mm, D:15mm) ve $S7_{490}$ (a:30°, h:40mm, D:15mm) nolu numunelerde 'h' bindirme mesafesinin çekme kuvvetine etkisi

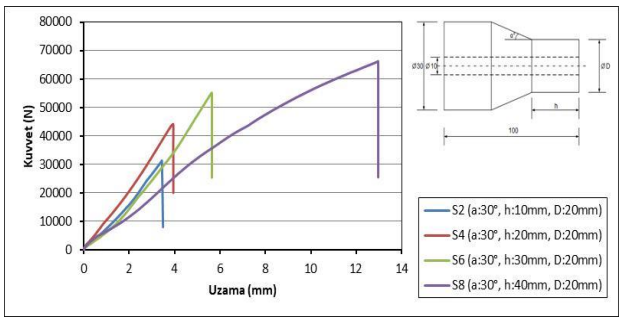

Şekil 8. DP490 yapıştırıcı kullanarak birleştirilen $S2_{490}$ (a:30°, h:10mm, D:20mm), $S4_{490}$ (a:30°, h:20mm, D:20mm), $S6_{490}$ (a:30°, h:30mm, D:20mm) ve $S8_{490}$ (a:30°, h:40mm, D:20mm) nolu numunelerde 'h' bindirme mesafesinin çekme kuvvetine etkisi

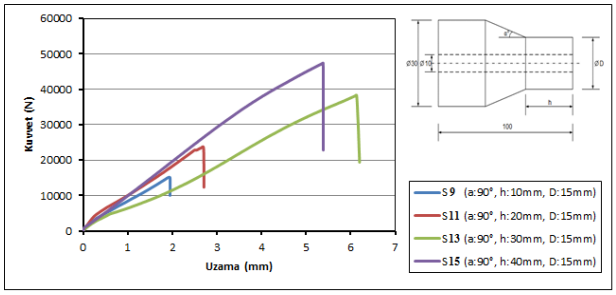

Şekil 9. DP490 yapıştırıcı kullanarak birleştirilen $S9_{490}$ (a:90°, h:10mm, D:15mm), $S11_{490}$ (a:90°, h:20mm, D:15mm), $S13_{490}$ (a:90°, h:30mm, D:15mm) ve $S15_{490}$ (a:90°, h:40mm, D:15mm) nolu numunelerde 'h' bindirme mesafesinin çekme kuvvetine etkisi

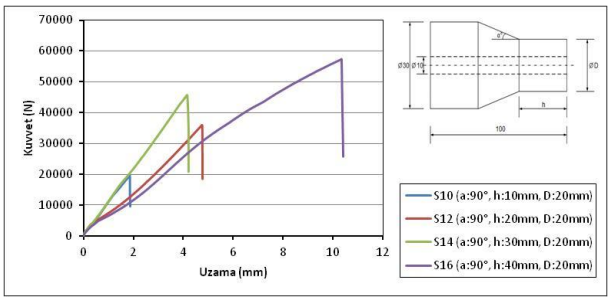

Şekil 10. DP490 yapıştırıcı kullanarak birleştirilen $S10_{490}$ (a:90°, h:10mm, D:20mm), $S12_{490}$ (a:90°, h:20mm, D:20mm), $S14_{490}$ (a:90°, h:30mm, D:20mm) ve $S16_{490}$ (a:90°, h:40mm, D:20mm) nolu numunelerde 'h' bindirme mesafesinin çekme kuvvetine etkisi

Çekme kuvvet değerleri incelendiği, maksimum ve minimum çekme kuvveti değerleri $S8_{490}$ (a:30° , h:40mm, D:20 mm) ve $S9_{490}$ (a:90° , h:10mm, D:15 mm) numunelerin de sırasıyla 66183,59 N ve 15054,69 N olarak elde edilmiştir. Bu durumun h bindirme mesafesinin artmasına paralel olarak yapışma yüzey alanın artmasına bağlı olduğu düşünülmektedir.

3.3 DP410 ile Birleştirilen Numunelerde 'a' Bindirme Açısının Çekme Kuvvetine Etkisinin İncelenmesi

DP 410 kullanılarak birleştirilen halka kesitli çubuklarda parametrelerden a açısının etkisi incelenmiştir. İki farklı bindirme açısının kıyaslandığında; DP410 yapıştırıcısı ile iki farklı bindirme açısı (30°, 90°) kullanılarak halka kesitli çubuklar birleştirilmiştir. Yapılan birleştirmelerde a bindirme açısının çekme yükü altındaki davranışları incelenmiştir. Numunelerin çekme kuvvetleri altındaki davranışları incelendiğinde a bindirme açısı artıkça çekme yükünün azaldığı görülmüştür. Çekme kuvvet değerleri incelendiği, maksimum ve minimum çekme kuvveti değerleri $S8_{410}$ (a:30°, h:40mm, D:20 mm) ve $S9_{410}$ (a:90°, h:10mm, D:15 mm) numunelerin de sırasıyla 104226.6 N ve 35328,13 N olarak elde edilmiştir. Genel olarak a bindirme açısının artmasına bağlı olarak yapışma yüzey alanın azalmasına ve çekme kuvvetinin azalmasına neden olduğu görülmektedir.

3.4 DP490 ile Birleştirilen Numunelerde 'a' Bindirme Açısının Çekme Kuvvetine Etkisinin İncelenmesi

DP490 kullanılarak birleştirilen halka kesitli çubuklarda parametrelerden a açısının etkisi incelendiğinde; DP490 yapıştırıcısı ile iki farklı bindirme açısı(30° ve 90°) kullanılarak halka kesitli çubuklar birleştirilmiştir. Yapılan birleştirmelerde a bindirme açısının çekme yükü altındaki davranışları incelenmiştir. Numunelerin çekme kuvvetleri altındaki davranışları incelendiğinde a bindirme açısı artıkça çekme yükünün azaldığı görülmüştür. Çekme kuvvet değerleri incelendiği, maksimum ve minimum çekme kuvveti değerleri $S8_{490}$ (a:30°, h:40mm, D:20 mm) ve $S9_{490}$ (a:90°, h:10mm, D:15 mm) numunelerin de sırasıyla 66183,59 N ve 15054,69 N olarak elde edilmiştir. Genel olarak a bindirme açısının artmasına bağlı olarak yapışma yüzey alanın azalmasına ve çekme kuvvetinin azalmasına neden olduğu düşünülmektedir.

3.5 DP410 ile Birleştirilen Numunelerde 'h' Bindirme Mesafesinin Burulma Açısına Etkisinin İncelenmesi

JİNAN NDW-200 marka ve maksimum çalışma torku 170 N.m olan burulma cihazında yapılan burulma deneylerinde numuneler deneyler sonucunda hasara uğramamıştır. Bunun için burulma torkunu 70 N.m seçerek bu torka denk gelen burulma açılarını numuneler arasında değerlendirilmiştir. DP410 kullanılarak birleştirilen halka kesitli çubuklarda h bindirme mesafesinin burulma açısına etkisi incelenmiştir. Dört farklı bindirme mesafesinin (10mm, 20mm, 30mm, 40mm) kıyaslanmasıyla oluşturulan grafikler Şekil 11, 12, 13 ve 14'te gösterilmiştir.

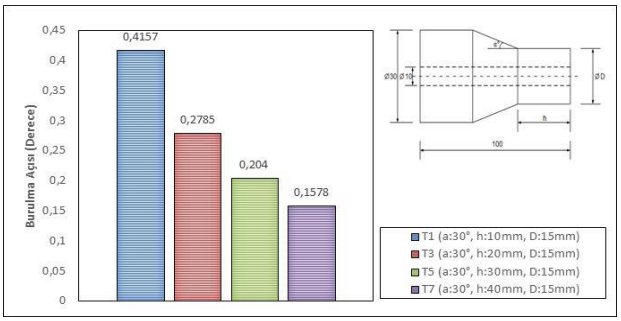

Şekil 11. DP410 yapıştırıcı kullanarak birleştirilen $T1_{410}$ (a:30°, h:10mm, D:15mm), $T3_{410}$ (a:30°, h:20mm, D:15mm), $T5_{410}$ (a:30°, h:30mm, D:15mm) ve $T7_{410}$ (a:30°, h:40mm, D:15mm) nolu numunelerde 'h' bindirme mesafesinin burulma açısına etkisi

DP410 yapıştırıcısı kullanılarak dört farklı (10mm, 20mm, 30mm, 40mm) h bindirme mesafelerinde halka kesitli çubukların birleştirilmesi yapılmıştır. Yapılan birleştirmelerde h bindirme mesafesinin burulma açısına

etkisini incelemek için DP410 ile birleştirilmiş numuneler burulmaya maruz bırakılmıştır.

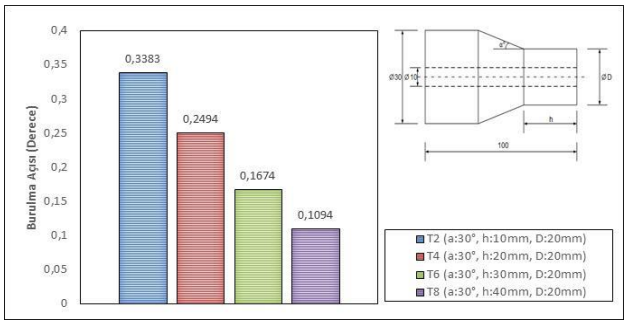

Şekil 12. DP410 yapıştırıcı kullanarak birleştirilen $T2_{410}$ (a:30º, h:10mm, D:20mm), $T4_{410}$ (a:30º, h:20mm, D:20mm), $T6_{410}$ (a:30º, h:30mm, D:20mm) ve $T8_{410}$ (a:30º, h:40mm, D:20mm) nolu numunelerde 'h' bindirme mesafesinin burulma açısına etkisi

Numunelerin burulma altındaki davranışları incelendiğinde genel olarak h bindirme mesafesi artıkça burulma açısının azaldığı görülmüştür. Burulma açısı değerleri incelendiğinde, maksimum ve minimum burulma açıları $T9_{410}$ ve $T8_{410}$ nolu numuneler de sırasıyla 0,8334º ve 0,1094º olarak elde edilmiştir. Bu durumun h bindirme mesafesinin artmasına paralel olarak yapışma yüzey alanın artmasına bunun bağlantı mukavemetini arttırması ve burulma açısının azalmasına sebep olduğu görülmüştür.

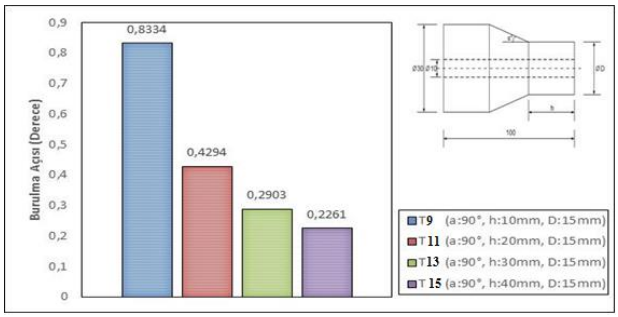

Şekil 13. DP410 yapıştırıcı kullanarak birleştirilen $T9_{410}$ (a:90º, h:10mm, D:15mm), $T11_{410}$ (a:90º, h:20mm, D:15mm), $T13_{410}$ (a:90º, h:30mm, D:15mm) ve $T15_{410}$ (a:90º, h:40mm, D:15mm) nolu numunelerde 'h' bindirme mesafesinin burulma açısına etkisi

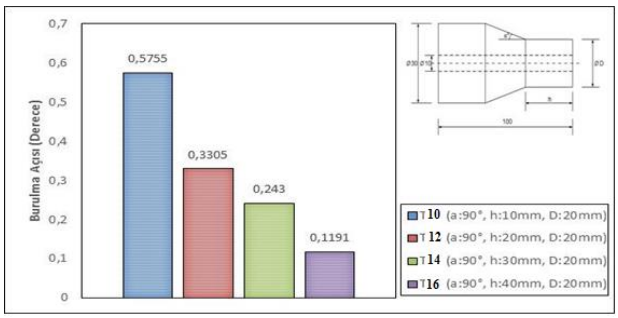

Şekil 14. DP410 yapıştırıcı kullanarak birleştirilen $T10_{410}$ (a:90º, h:10mm, D:20mm), $T12_{410}$ (a:90º, h:20mm, D:20mm), $T14_{410}$ (a:90º, h:30mm, D:20mm) ve $T16_{410}$ (a:90º, h:40mm, D:20mm) nolu numunelerde 'h' bindirme mesafesinin burulma açısına etkisi

3.6 DP490 ile Birleştirilen Numunelerde 'h' Bindirme Mesafesinin Burulma Açısına Etkisinin İncelenmesi

DP490 kullanılarak birleştirilen halka kesitli çubuklarda h bindirme mesafesinin burulma açısına etkisi incelenmiştir. Dört farklı bindirme mesafesinin (10mm, 20mm, 30mm, 40mm) kıyaslanmasıyla oluşturulan grafikler Şekil 15, 16, 17 ve 18'de verilmiştir.

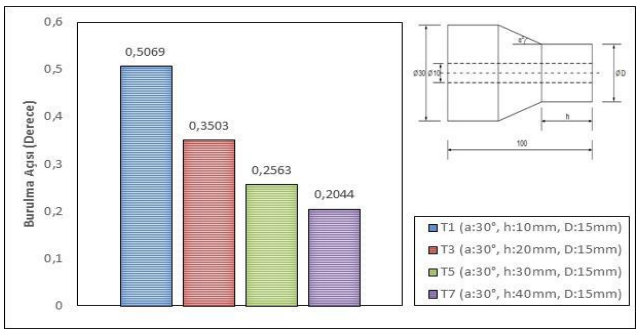

Şekil 15. DP490 yapıştırıcı kullanarak birleştirilen $T1_{490}$ (a:30º, h:10mm, D:15mm), $T3_{490}$ (a:30º, h:20mm, D:15mm), $T5_{490}$ (a:30º, h:30mm, D:15mm) ve $T7_{490}$ (a:30º, h:40mm, D:15mm) nolu numunelerde 'h' bindirme mesafesinin burulma açısına etkisi

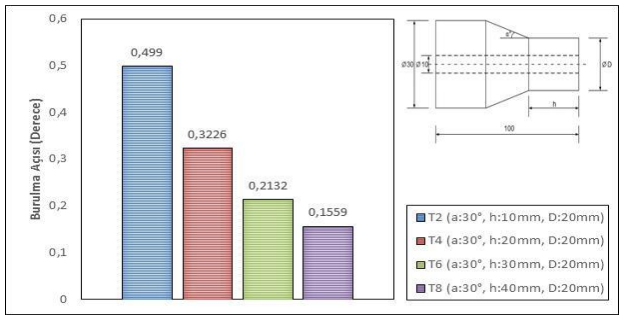

Şekil 16. DP490 yapıştırıcı kullanarak birleştirilen $T2_{490}$ (a:30º, h:10mm, D:20mm), $T4_{490}$ (a:30º, h:20mm, D:20mm), $T6_{490}$ (a:30º, h:30mm, D:20mm) ve $T8_{490}$ (a:30º, h:40mm, D:20mm) nolu numunelerde 'h' bindirme mesafesinin burulma açısına etkisi

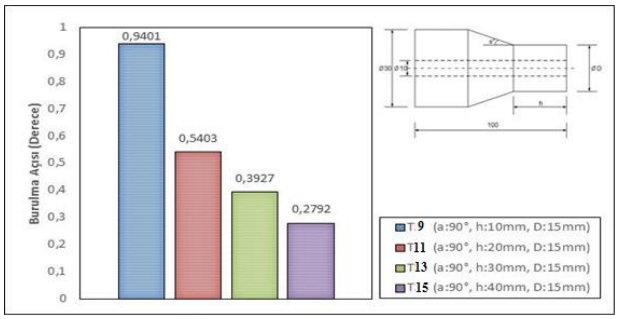

Şekil 17. DP490 yapıştırıcı kullanarak birleştirilen $T9_{490}$ (a:90º, h:10mm, D:15mm), $T11_{490}$ (a:90º, h:20mm, D:15mm), $T13_{490}$ (a:90º, h:30mm, D:15mm) ve $T15_{490}$ (a:90º, h:40mm, D:15mm) nolu numunelerde 'h' bindirme mesafesinin burulma açısına etkisi

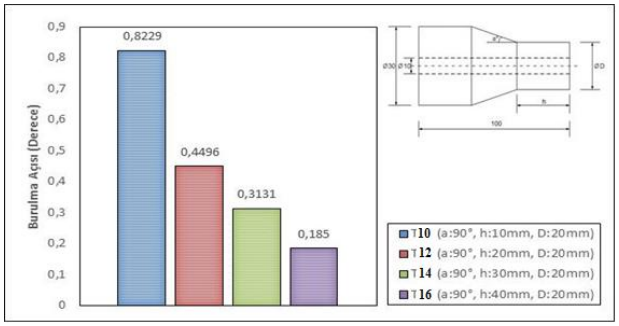

Şekil 18. DP490 yapıştırıcı kullanarak birleştirilen $T10_{490}$ (a:90º, h:10mm, D:20mm), $T12_{490}$ (a:90º, h:20mm, D:20mm), $T14_{490}$ (a:90º, h:30mm, D:20mm) ve $T16_{490}$ (a:90º, h:40mm, D:20mm) nolu numunelerde 'h' bindirme mesafesinin burulma açısına etkisi

DP490 yapıştırıcısı kullanılarak dört farklı (10mm, 20mm, 30mm, 40mm) h bindirme mesafelerinde halka kesitli çubukların birleştirilmesi yapılmıştır. Yapılan birleştirmelerde h bindirme mesafesinin burulma açısına etkisini incelemek için DP490 ile birleştirilmiş numuneler burulmaya maruz bırakılmıştır. Numunelerin burulma altındaki davranışları incelendiğinde genel olarak h bindirme mesafesi artıkça burulma açısının azaldığı görülmüştür. Burulma açısı değerleri incelendiğinde, maksimum ve minimum burulma açıları $T9_{490}$ ve $T8_{490}$ nolu numuneler de sırasıyla 0,9401^o ve 0,1559^o olarak elde edilmiştir. Bu durumda h bindirme mesafesinin artışıyla burulma açılarında azalma meydana gelmiştir. Bunun sebebi mesafe artışıyla yüzey alanında artış olmaktadır ve bu durumun bağlantı mukavemetini yükseltirken burulma açısında azalmaya sebep olmuştur.

4 Sonuçlar

Bu çalışmada; halka kesitli çubukların birleştirilmesinde çevresel yapışma yüzeyinin bağlantı mukavemetine etkisini incelemek için iki farklı özelliğe sahip yapıştırıcı (DP410 ve DP490) dört farklı bindirme mesafesi (10, 20, 30 ve 40 mm), iki farklı bindirme açısı (30^o ve 90^o) ve farklı bindirme iç açısına sahip parçalar farklı parametrelerde birleştirilip çekme ve burulma deneylerine tabi tutulmuştur. Deneysel çalışma ile elde edilen sonuçlar aşağıda verilmiştir.

1. Birleştirmelerin çekme kuvvetleri altındaki davranışları incelendiğinde genel olarak h bindirme mesafesi artıkça çekme yükünün arttığı ve a açısı arttıkça çekme yükünün azaldığı görülmüştür.
2. Çekme kuvvet değerleri incelendiği, maksimum ve minimum çekme kuvveti değerleri $S8_{410}$ ve $S9_{410}$ nolu numuneler de sırasıyla 104226,6 N ve 35328,13 N olarak elde edilmiştir.
3. DP410 yapıştırıcıyla yapıştırılan numunelerin burulma deneyleri de yapılmıştır. Burulma deneyleri incelendiğinde ise maksimum burulma açısı $T9_{410}$ numunesinde 0,8334^o ve minimum burulma açısı $T8_{410}$ num unede 0,1094^o derece olarak gözlemlenmiştir. Bu durumun h bindirme mesafesinin artmasına paralel olarak yapışma yüzey alanın artmasına, a bindirme çapının artışıyla yüzey alanı azalmasına bağlı olarak değişim göstermişitr.
4. Yapılan birleştirmelerde DP490 ile birleştirilmiş numunelerin çekme deneyleri yapılmıştır. Belirlenen parametreler ışığında deneyleri yapılan numunelerin çekme davranışları incelendiğinde h bindirme mesafesi artışıyla çekme kuvvetleri artarken, a bindirme çapının artışıyla çekme kuvvetinde azalma gözlemlenmiştir. Çekme deneyleri neticesinde maksimum çekme kuvveti $S8_{490}$ numunesinde 66183,59 N ve minimum çekme kuvveti $S9_{490}$ numunede 15054,69 N elde edilmiştir.
5. DP490 yapıştırıcısıyla yapıştırılan numunelerin burulma deneyleri neticesinde elde edilen burulma açıları incelenmiştir. Maksimum ve minimum burulma açıları sırasıyla $T25_{490}$ numunesinde 0,9401^o ve $T8_{490}$ numunesinde 0,1559^o gözlemlenmiştir. Elde edilen veriler değerlendirildiğinde numunelerde yüzey alanlarında artış bağlantı mukavemetine olumlu yönde etki gösterdiği düşünülmektedir.
6. İki farklı yapıştırıcıyla birleştirilen halka kesitli çubukların çekme deneyleri neticesinde kullanılan yapıştırıcıların bağlantı mukavemetine etkisi incelendiğinde; DP410 yapıştırıcısıyla yapıştırılan numunelerin DP490 yapıştırıcısıyla yapıştırılan numunelere göre çekme kuvveti değerleri daha yüksek çıkmıştır. Burulma davranışları açısından da DP410 yapıştırıcısıyla yapıştırılan numunelerin DP490 yapıştırıcısıyla yapıştırılan numunelere göre daha iyi davranış göstermiştir.

5 Teşekkür

Bu çalışma Bingöl Üniversitesi Bilimsel Araştırmalar Birimi Tarafından BAP-MMF.2018.00.003 nolu proje kapsamından desteklenmiştir. Katkılarından dolayı Bingöl Üniversitesi BAP birimine teşekkür ederiz.

Kaynaklar

[1] Solmaz, M.Y., Turgut, A., An Experimental and Numerical Study on the Effects of Taper Angles and Overlap Length on the Failure and Stress Distribution of Adhesively-Bonded Single-Lap Joints, The 1st International Symposium on Computing in Science & Engineering (ISCSE), June, 3-5, p. 866-874, Kusadasi, Aydin, 2010.

[2] Solmaz M.Y., Yapıştırıcı İle Birleştirilmiş Bağlantıların Mekanik Analiz ve Tasarımları, Doktora Tezi, Fırat Üniversitesi Fen Bilimleri Enstitüsü, Elazığ, 2008.

[3] Taş B., Yapıştırıcı İle Birleştirilmiş Konik Geçmeli Bağlantıların Burulma Momenti Altındaki Performansları, Yüksek Lisans Tezi, Fırat Üniversitesi Fen Bilimleri Enstitüsü, Elazığ, 2016.

[4] Hur, S.H., Son, H.J., Kweon, J. H., Choi, J.H., Postbuckling of composite cylinders under external hydrostatic pressure, Composite Structures, 2008.

[5] Tafresi, A., Bailey C. G., Instability of imperfect composite cylindrical shells under combined loading, Composite structures 80, 49-64, 2007.

[6] Yang, C., Huang, H., Guan, Z., Stress Model of Composite Pipe Joints under Bending, Journal of Composite Materials, 36, 1331, 2002.

[7] Gül A., Yapıştırma bağlantılı kompozit boruların burkulma analizi, Yüksek Lisans Tezi, Atatürk Üniversitesi Fen Bilimleri Enstitüsü, Erzurum, 2013.

[8] Aimmanee S., Hongpimolmas P., Stress analysis of adhesive-bonded tubular-coupler joints with optimum variable-stiffness composite adherend under torsion, composite structures 164,76-89, 2017.

[9] Oh J.H., torque capacity of tubular adhesive joints with different composite adherends, materials letters 62, 1234-1237, 2008.

[10] Jeroen Van, W., Jan De, P., Patrick De, B., Wim De, W., Magd A.W., Guido De, R., Experimental determination of the fatigue life of modified threaded pipe couplings, Procedia Engineering 2,1849-1858, 2010.

[11] Vaziri A., Nayeb-Hashemi H., Dynamic response of tubular joints with an annular void subjected to a harmonic axial load, International Journal of Adhesion and Adhesives 22, 367-373, 2002.

[12] Das R.R., Baishya N., Failure Analysis of Bonded Composite Pipe joints subjected to internal Pressure and Axial loading, Procedia Engineering, 1047-1054, 2016.
[13] Li, H., Zhang, X., Qi, D., Cai, X., Ding, N., Wei, B., Qi, G., Failure analysis of the adhesive metal joint bonded on anticorrosion plastic alloy composite pipe, Engineering Failure Analysis 47,49-45, 2015.
[14] Rohem, N.R.F., Pacheco, L.J., Budhe, S., Banea, M.D., Sampaio, E.M., de Barros, S., Development and qualification of a new polymeric matrix laminated composite for pipe repair, Composite Structures 152, 737-745, 2016.
[15] Liu, J., Qin, M., Zhao, Q., Chen., Liu, P., Gao, J., Fatigue performances of the cracked aluminum-alloy pipe repaired with a shaped CFRP patch, Thin-Walled Structures111, 155-164, 2017.

International Journal of Innovative Engineering Applications

Journal homepage: https://dergipark.org.tr/ijiea

DETERMINING THE EFFICIENCY OF MASS TRAPPING OF YELLOW STICKY TRAPS IN DIFFERENT WAVELENGTHS AGAINS PISTACHIO PSYLLID IN SİİRT PROVINCE [*Agonescena pistaciae* Burc. and Laut. (Hemiptera: Psyllidae)]

İnanç Özgen[1]*, Halil Bolu[2], Tarkan Ayaz[3], İbrahim Koç[4],Çetin Mutlu[5], Ayçin Aksu Altun[6]

[1]*Fırat University, Engineering Faculty, Bioengineering Department, Turkey*
[2]*Dicle University, Agricultural Faculty, Plant Protection Department, Turkey*
[3]*Şırnak University, Agricultural Faculty, Plant Protection Department, Turkey*
[4]*Bitlis Eren University, Faculty of Engineering and Architecture, Environmental Engineering Department, Turkey*
[5]*Harran University, Agricultural Faculty, Plant Protection Department, Turkey*
[6]*GAP Agricultural Research Institute, Turkey*

Abstract

Original scientific paper

This study was conducted in gardens infested with pistachio psylla in Siirt Province between 2007 and 2010. It was detected that pistachio psylla forms were the highest populations in the pistachio gardens in the Central District of Siirt Province. It causes important damages particularly on young leaves in mid-June and in the maturing period of fruits in mid- and late-August. The yellow sticky trap coded 1016 B was found to be more effective than other coded traps. It was concluded that these traps were important for decreasing of the population of the pest in cases where the population is low. It was found that traps provided positive contribution if combined with other control methods. One of the best promising results was gathered when used in 4 traps for each tree and 7-day periods of hanging

Keywords: *Agonescena pistaciae, Population, Trap Numbers, IPM*

1 Introduction

One of the most important problems in the production of Pistachio is related to protection of the plant against pest insects. Pistachio psylla *Agonescena pistaciae* Burchardt & Lauterer,1989 (Hemiptera: Psyllidae) is among the most important species as regards the economy (Altın et al., 1992; Altın et al., 1996; Bolu, 2002). Chemicals are used in general against the pistachio psylla, *A. pistaciae*, and use of chemical at wrong times and wrong dosages create negative results on the agroecosystem. Conventional methods used against the pistachio psylla, which cause significant economic losses in pistachio cultivation lands in the Southeastern Anatolia Region in Turkey, are not sufficient per se to remove the pest problem. One of the principle trends of the pests for is to use light and color traps as a method of combat against pests. This method is also useful to determine the timing for control of pests. In general, yellow-colored traps are used to make the insects for mass trapping. Furthermore, they are used both as a direct and indirect fighting method (Öncüer, 2000). It was reported that in addition to the high reflection values of the yellow color, yellow-colored objects create higher-than-normal stimulations on insects, in other words, all the phytophage insects are attracted by the yellow color. Together with the high reflection amounts of the yellow color, it was also reported that yellow objects attract insects in levels higher than normal, in other words, all the phytophage insects are attracted with the yellow color (Hirato and Kato, 2011).

Again, some other investigators have used yellow sticky traps to determine the density of adult population of pistachio psylla and its reproduction rate. It has been concluded that yellow adhesive traps were important for seasonal population studies (Hadiyan and Seyedoleslami, 2001). In their study, they determined the efficiency of yellow adhesive traps with different RAL codes and, Özgen et al. (2013) used yellow sticky traps in 8 different tones, and determined that code 1016 attracted psylla adults more and among the variations of the yellow color, code. This study was implemented with the purpose of determining the efficiency of attraction of psylla in populations with different adult densities by code 1016 B with high attraction power.

2 Material and Method

2.1 Material

The main materials of the study consisted of pistachio trees in Siirt Province, *A. pistaciae*, yellow sticky traps in different wavelengths, japenese umbrella, ice cups, Petri dishes in different sizes, and similar.

2.2 Method

* Corresponding author.
E-mail address: inancozgen@gmail.com (İ. Özgen) | ORCID Number : 0000-0003-1742-9324
Received 15 May 2020; Received in revised form 9 June 2020; Accepted 18 June 2020
2587-1943 | © 2020 IJIEA. All rights reserved. Doi:

2.2 Method

In the follow-up of the population of the pest, 10 compound leaves were collected from in different directions from each tree in each garden starting with the foliation of tress, periods of adulthood, nymph and egg periods of the pest were traced. Follow-up of populations of the natural enemies of the pest in sampling gardens was carried out by making the beneficial insects onto the japenese umbrella by hitting the trees on four sides; and also, natural enemy species were counted by capturing on yellow adhesive traps. After counting and releasing the known insect species dropping onto the japenese umbrella, other insects were taken into the killing bottle; when these insects were thus killed, they were taken into Petri dishes containing blotting paper, and were brough to the laboratory. The following methods were applied as of the years of the study. As mentioned in the methods section, 10 compound leaves were collected from each tree in each garden starting from the time of emerging of the pest in nature, and adult, nymph and egg stages of the pest were followed on 100 leaves in total. These procedures were carried out using loops with the purpose of not decreasing the pest population, through collection of leaves. In total, 50 yellow adhesive traps were hanged on 20 trees in total (1 trap on 5 trees, 2 traps on 5 trees, 3 traps on 5 trees, and 4 traps on 5 trees) in this period with the purpose of reducing the pest population. Furthermore, 3 trees were left without traps for comparison. Traps were counted with weekly intervals and adult individuals were recorded.

3 Results

In previously study; The yellow sticky trap coded 1016 B was found to be more effective than other coded traps (Özgen et al., 2013).Because of the trap coded 1016 was found statistically more effective as compared to the other traps, in this study a trial was set based on the lightening of color on the trap coded 1016, and following the application, and results on days 1, 4 and 7 are shown in Figures 1, 2 and 3. Upon statistical examination of the study results, it was seen that trap coded 1016 B differed from the group of other traps, and captured the greatest number of adult individuals (Table 1). When the numbers of adult individuals captured in traps were considered as regards days, it was seen that days 1, 4 and 7 constituted different groups, and the traps that captured the greatest numbers of adult individuals were those counted in day 7 (Table 2).

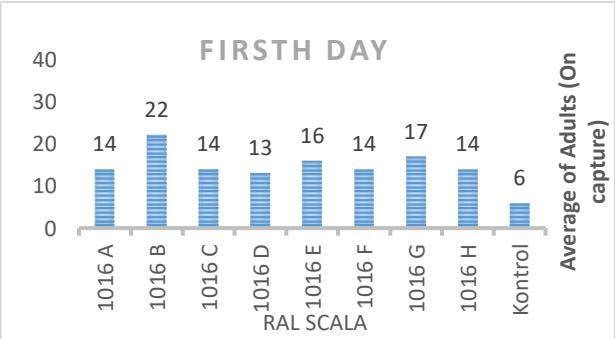

Figure 1. Determination of different 1016 codes capture activities on the 1st day of application.

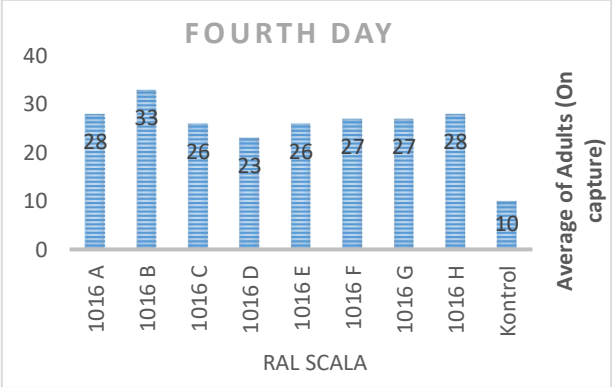

Figure 2. Determination of different 1016 codes capture activities on the 4th day of application.

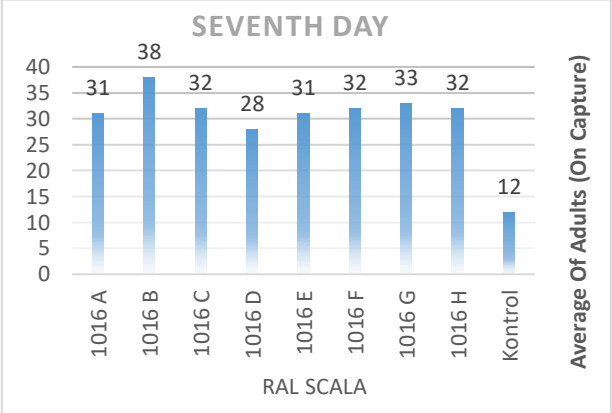

Figure 3. Determination of different 1016 codes capture activities on the 7th day of application.

Table 1. Statistical evaluation of different versions of trap 1016.

Level				Least Sq Mean
1016 B	A			31,000000
1016 G		B		25,666667
1016 H		B	C	24,666667
1016 A		B	C	24,333333
1016 E		B	C	24,333333
1016 F		B	C	24,333333
1016 C		B	C	24,000000
1016 D			C	21,333333
Control			D	9,333333

Table 2. Averages of adult individuals captured with traps on different days.

Level			Least Sq Mean
7	A		29,888889
4		B	25,333333
1		C	14,444444

3.1 Efficiency of Sticky Traps in Different Numbers (1, 3 and 4) on the Numbers of Adults and Nymphs in Two Different Population Densities

After determining the most suitable tone of yellow and hanging height, trap coded 1016 B was hanged on trees in different numbers (1 trap, 3 traps, and 4 traps), and differences between the numbers of adult individuals captured in traps and the effects of these numbers of nymphs on trees were determined.

3.2. Effects of Trap Numbers on the Psylla Adult Population on Two Different Population Densities (A and B) in Different Days

a. Population A

According to individual counts, the adult population was in the range of **26 and 38**. Numbers of adult individuals captured with trap numbers of 1, 3 and 4 are shown in Figures 4, 5 and 6.

b. Population B

It was found in the counts that the adult population was in the range of **38 and 46,** and study was carried out on this population. Numbers of adult individuals captured with trap numbers of 1, 3 and 4 are shown in Figures 7, 8 and 9.

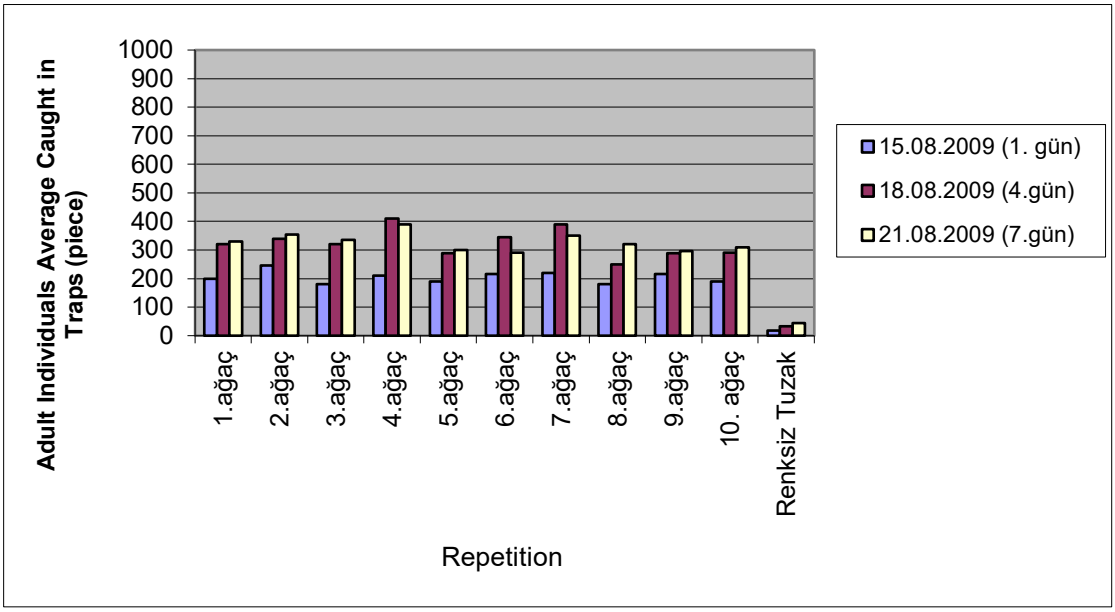

Figure 4. Number of Adult Individuals Captured on One Sticky Trap on Trees on Day 1st, 4th and 7th .

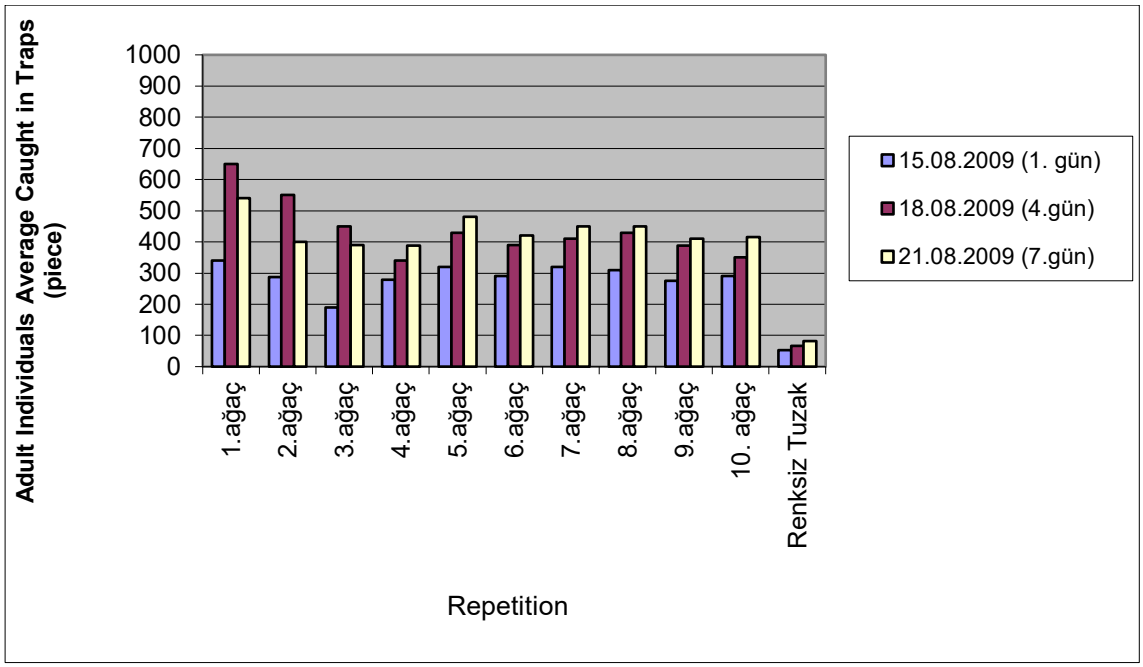

Figure 5. Number of Adult Individuals Captured on Three Sticky Traps on Trees on Day 1st, 4th and 7th .

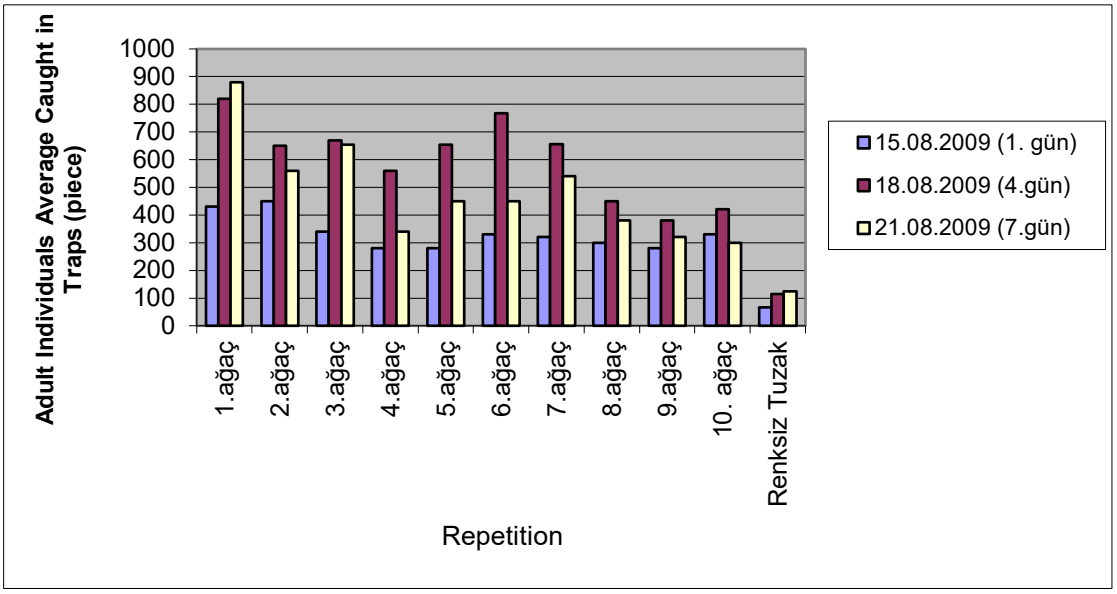

Figure 6. Number of Adult Individuals Captured on Four Sticky Traps on Trees on Day 1st, 4th and 7th .

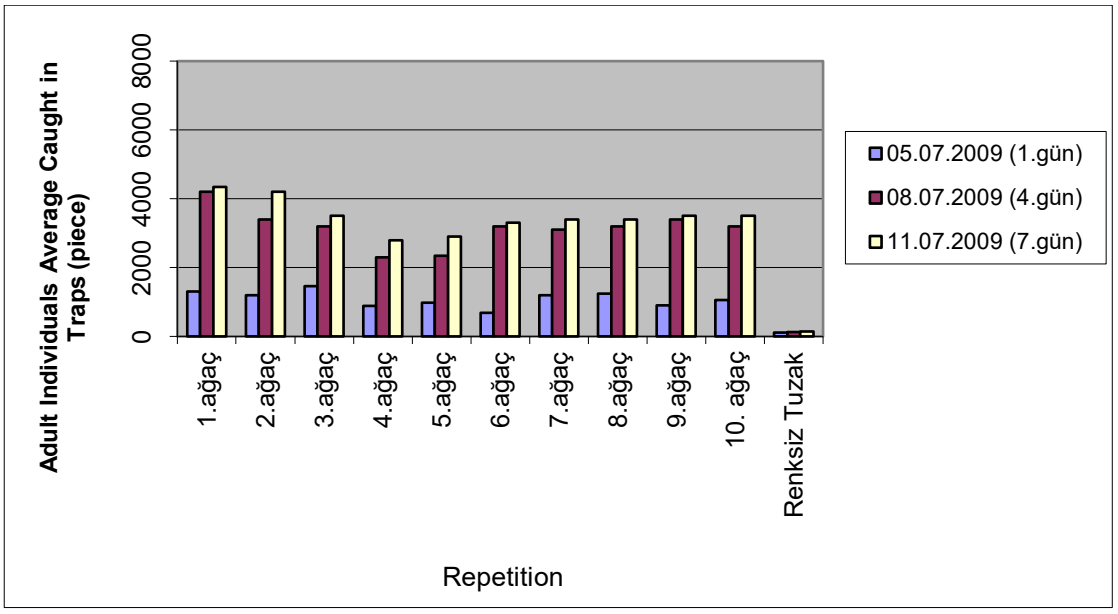

Figure 7. Number of Adult Individuals Caught on One Sticky Trap on Trees on Day 1st, 4th and 7th **.**

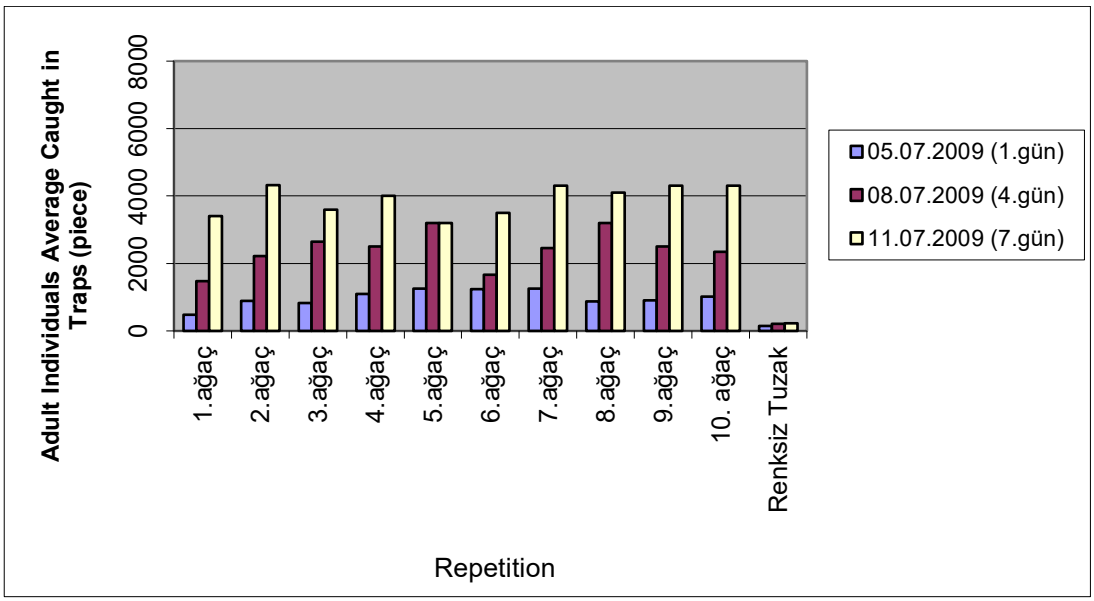

Figure 8. Number of Adult Individuals Caught on Three Sticky Traps on Trees on Day 1st, 4th and 7th **.**

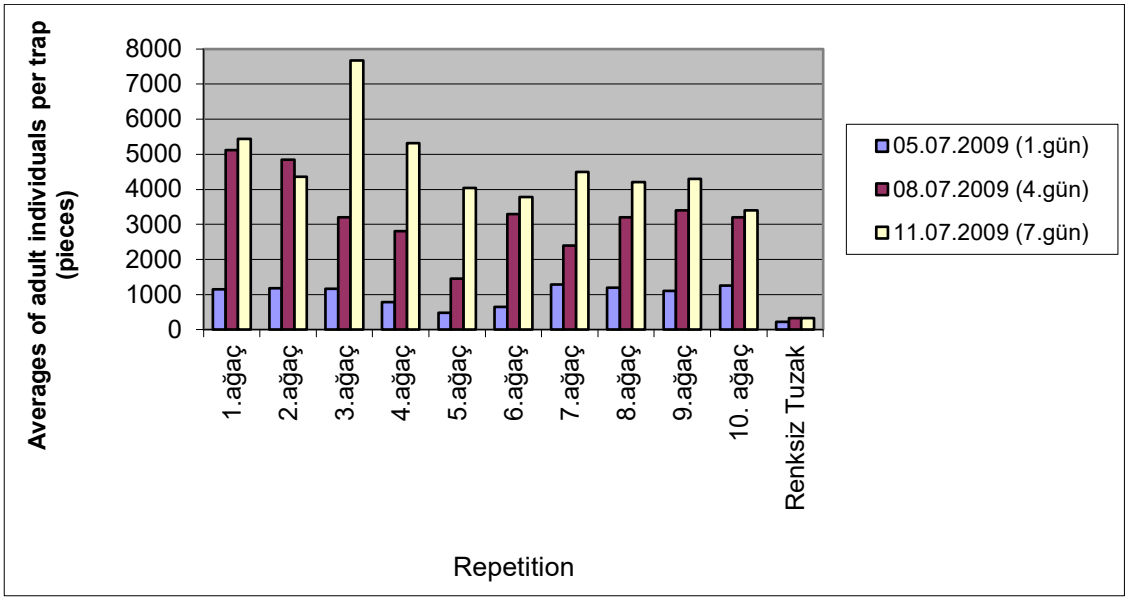

Figure 9. Number of Adult Individuals Caught on Four Sticky Traps on Trees on Day 1st, 4th and 7th .

Statistical analyses showed differences between populations (Table 3).

Table 3. Statistical Difference Between Populations.

B	A	2448,2626
A	B	353,9596

Again, statistical evaluation of the trap numbers in the study, it was found that the numbers of adult individuals captured in trees with 4 traps were different from those numbers in trees with 1 and 3 traps hung. Accordingly, numbers of adult individuals captured increased with the number of traps hung on each tree (Table 4).

Table 4. The Difference Between the Numbers of Sticky Traps on a Tree

Trap counts		Least Sq Mean
Quadruple Trap	A	1599,4545
Single Trap	B	1308,2121
Triple Trap	B	1295,6667

In parallel with the other study, differences between the number of individuals captured increased with the increasing number of days that traps were hung, and statistically significant differences were found between the number of individuals captured in days 1, 4 and 7 (Table 5).

Table 5. Statistical Differences Between the Time of Sticky Traps to Stay on Trees.

Level			Least Sq Mean
7th Day	A		2035,0909
4th Day		B	1563,7879
1st Day		C	604,4545

3.1.3 Determining the Effects of Sticky Traps in Different Populations in Different Numbers (1, 3, and 4) with Wedge Impact Method and Nymph Counting Method

In this study however, whether or not reduction in population could be achieved was investigated based on counts of adults and leaves with wedge impact method and nymph counts with the purpose of determining the effects of traps on adult and nymph populations on 4 different populations based on adult and nymph counts of psylla.

1. Studies by Sticky 1 (one) trap

a. Population A

Mean numbers of adult individuals captured with wedge impact method after counts on days 1, 4 and 7 when the adult population reached the range between **24 and 32** in population follow-up in trees are given in Figure 10.

b. Population B

Counts of nymphs achieved in days 1, 4 and 7 after hanging 1 trap per tree after the mean nymph count on 10 compound leaves reached **13 and 16 nymphs** in population follow-up on trees are given in Figure 11.

c. Population C

Counts of adult individuals achieved in days 1, 4 and 7 per tree obtained with wedge impact method after reaching adult population reached the range between **35 and 41** are given in Figure 12.

d. Population D

Counts of nymphs achieved in days 1, 4 and 7 after hanging 1 trap per tree after the mean nymph count on 10 compound leaves reached **25 and 34 nymphs** in population follow-up on trees are given in Figure 13.

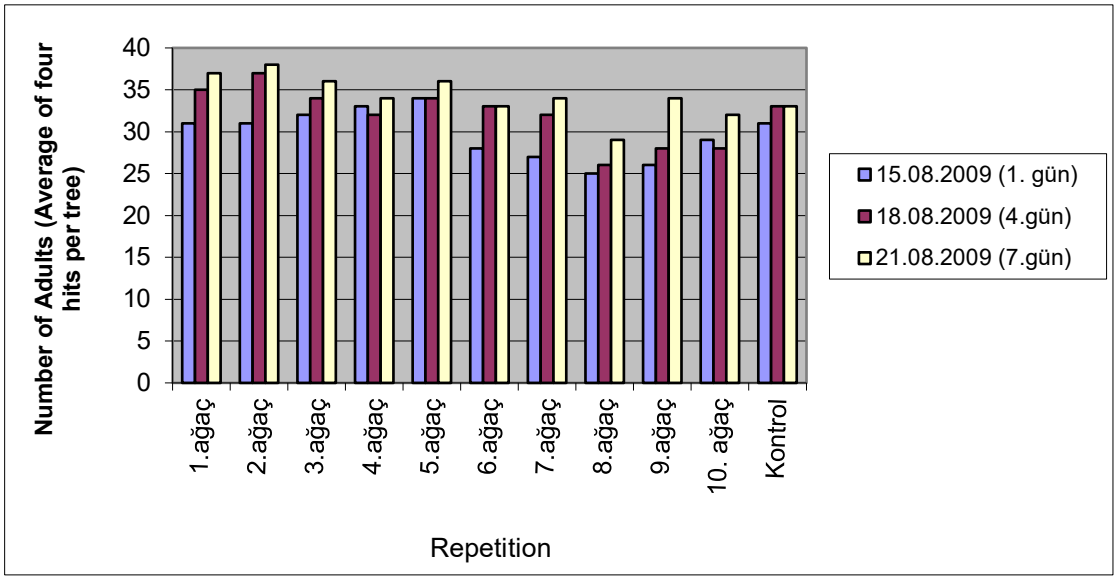

Figure 10. The effects of 1 (One) hang trap application per tree on adult population fluctuation of *Agonescena pistaciae* (between 24-32 adults) on days 1st, 4th and 7th.

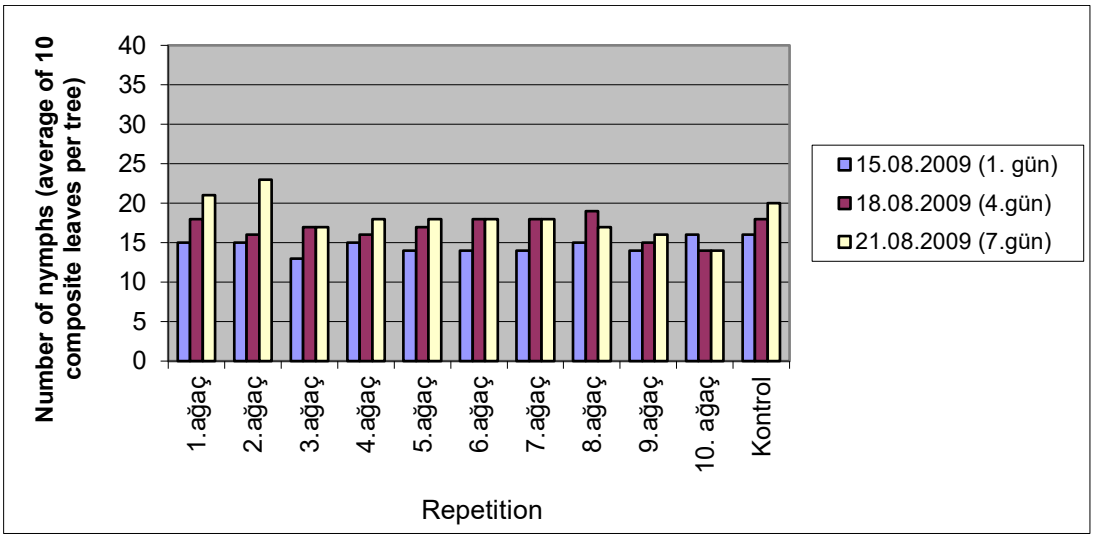

Figure 11. The effects of 1 (One) hang trap application per tree on nymph population fluctuation of *Agonescena pistaciae* (between 13-16 nymph) on days 1st, 4th and 7th.

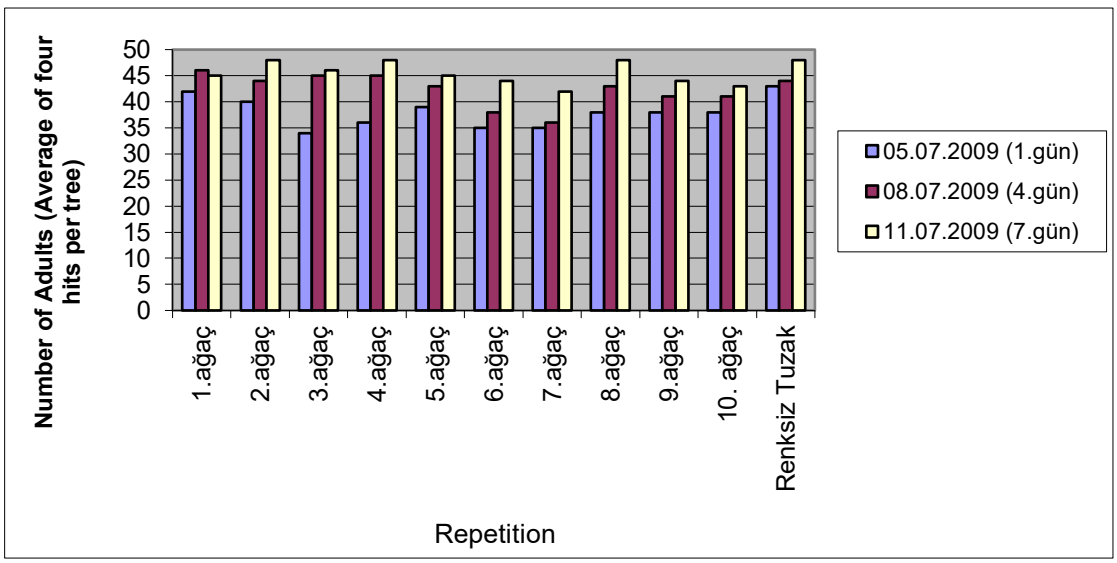

Figure 12. The effects of 1 (One) hang trap application per tree on adult population fluctuation of *Agonescena pistaciae* (between 35-41 adults) on days 1st, 4th and 7th.

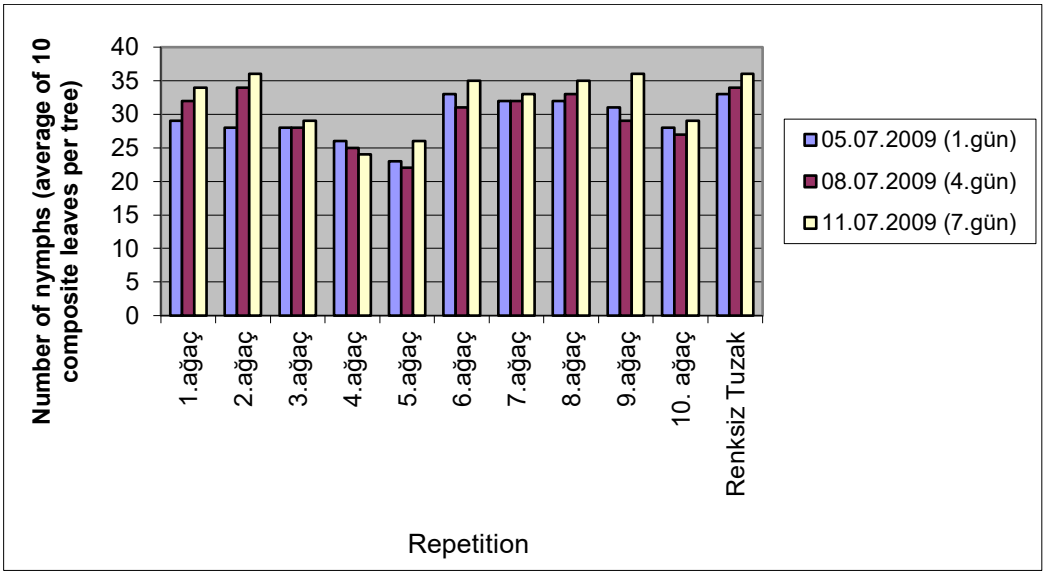

Figure 13. The effects of 1 (One) hang trap application per tree on nymph population fluctuation of *Agonescena pistaciae* (between 25-34 nymph) on days 1st, 4th and 7th.

2. Study with 3 Sticky traps

a. Population A

Counts of adult individuals achieved in days 1, 4 and 7 with three traps per tree obtained with wedge impact method after reaching adult population reached the range between **28 and 33** are given in Figure 14.

b. Population B

Counts of nymph individuals achieved in days 1, 4 and 7 with three traps per tree obtained with wedge impact method after reaching adult population reached the range between **14 and 15** on 10 compound leaves are given in Figure 15.

c. Population C

Counts of adult individuals achieved in days 1, 4 and 7 with three traps per tree obtained with wedge impact method after reaching adult population reached the range between 40 and 45 are given in Figure 16.

d. Population D

Counts of nymphs achieved in days 1, 4 and 7 after hanging 3 traps per tree after the mean nymph count on 10 compound leaves reached **27 and 33 nymphs** in population follow-up on trees are given in Figure 13.

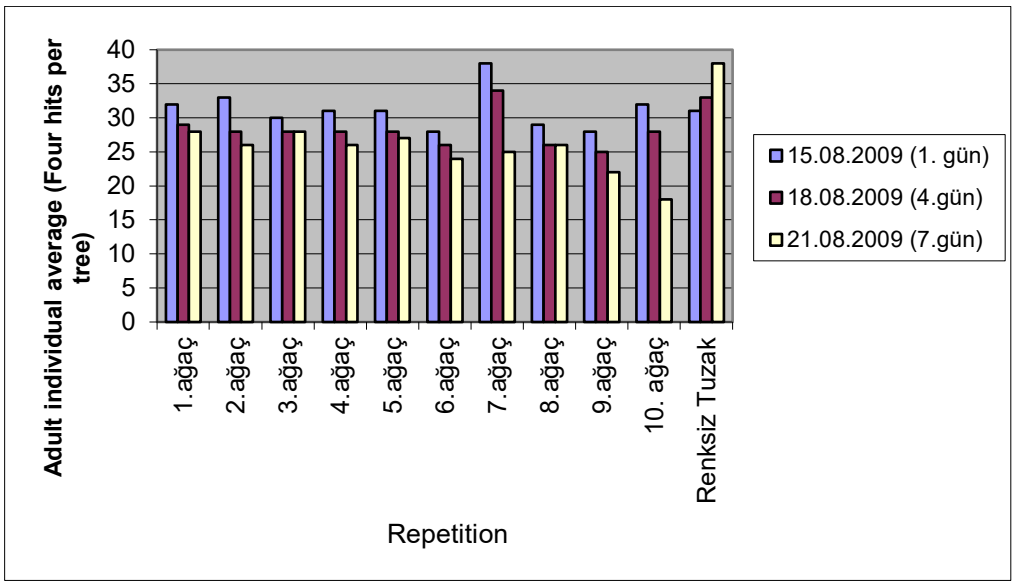

Figure 14. The effects of 3 (Three) hang trap application per tree on adult population fluctuation of *Agonescena pistaciae* (between 28-33 adults) on days 1st, 4th and 7th.

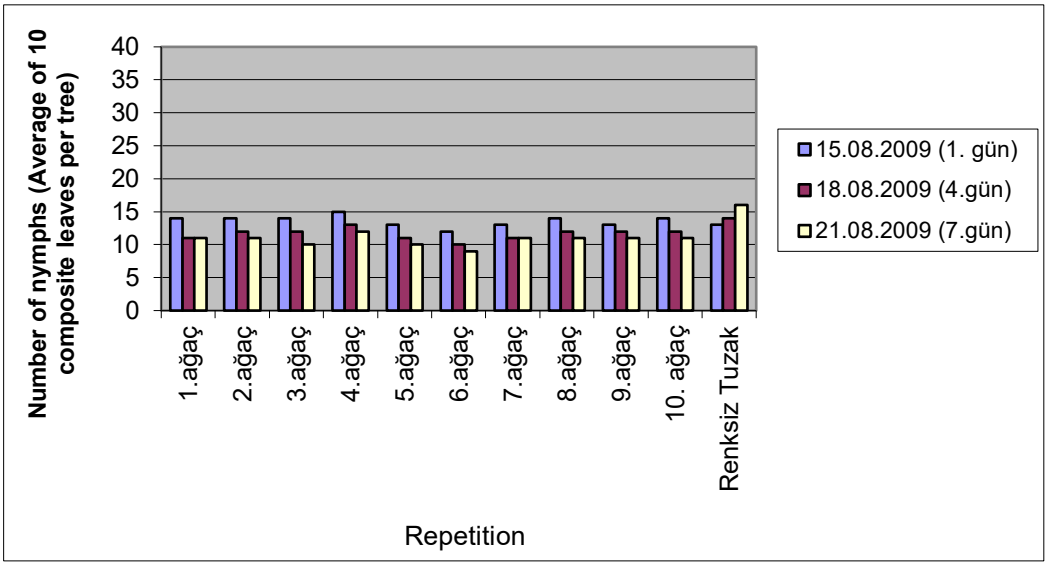

Figure 15. The effects of 3 (Three) sticky trap application per tree on nymph population fluctuation of *Agonescena pistaciae* (between 14-15 nymph) on days 1st, 4th and 7th.

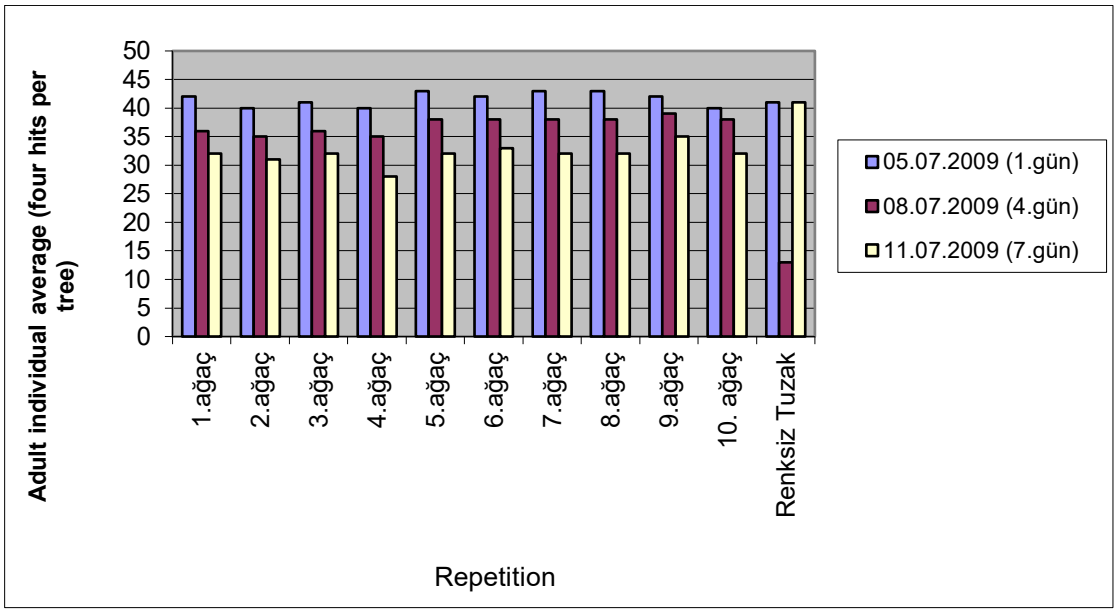

Figure 16. The effects of 3 (Three) hang trap application per tree on adult population fluctuation of *Agonescena pistaciae* (between 40-45 adults) on days 1st, 4th and 7th.

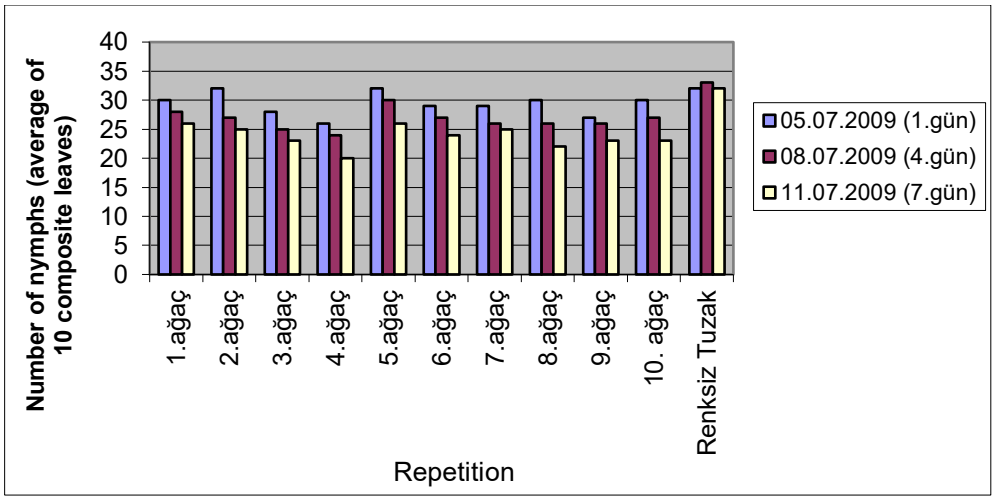

Figure 17. The effects of 3 (Three) hang trap application per tree on nymph population fluctuation of *Agonescena pistaciae* (between 27-33 nymph) on days 1st, 4th and 7th.

3. Study with 4 traps hung

a. Population A

Counts of adult individuals achieved in days 1, 4 and 7 with four traps per tree obtained with wedge impact method after the adult population reached the range between 26 and 38 are given in Figure 18.

b. Population B

Counts of nymphs achieved in days 1, 4 and 7 after hanging 4 traps per tree after the mean nymph count on 10 compound leaves reached 13 and 17 nymphs in population follow-up on trees are given in Figure 19.

c. Population C

Counts of adult individuals achieved in days 1, 4 and 7 with four traps per tree obtained with wedge impact method after the adult population reached the range between 36 and 46 are given in Figure 20.

d. Population D

Counts of nymphs achieved in days 1, 4 and 7 after hanging 4 traps per tree after the mean nymph count on 10 compound leaves reached 28 and 37 nymphs in population follow-up on trees are given in Figure 21.

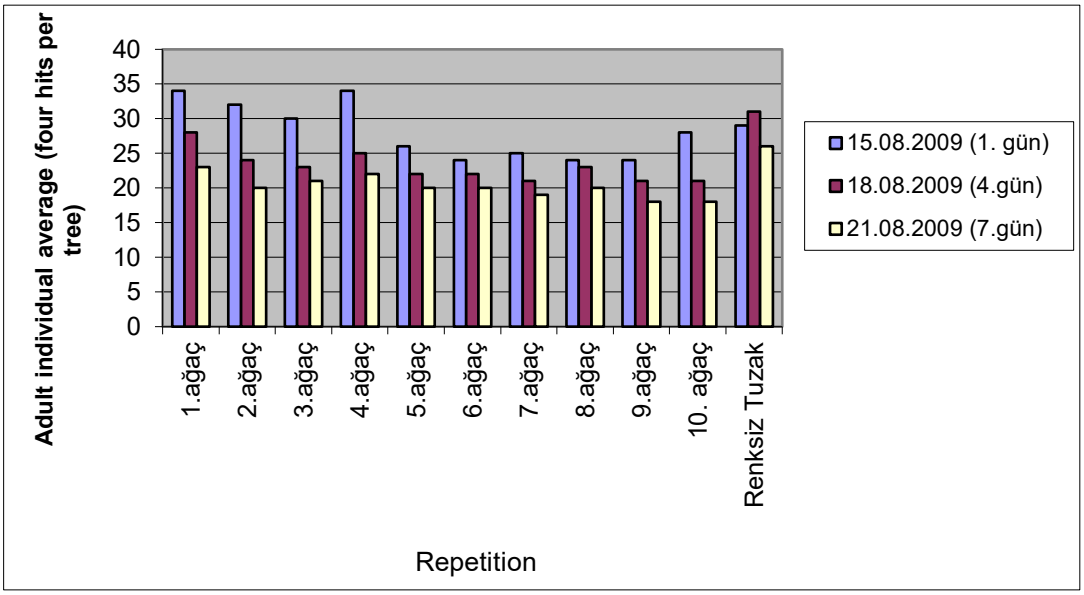

Figure 18. The effects of 4 (Four) hang trap application per tree on adult population fluctuation of *Agonescena pistaciae* (between 26-38 adults) on days 1st, 4th and 7th.

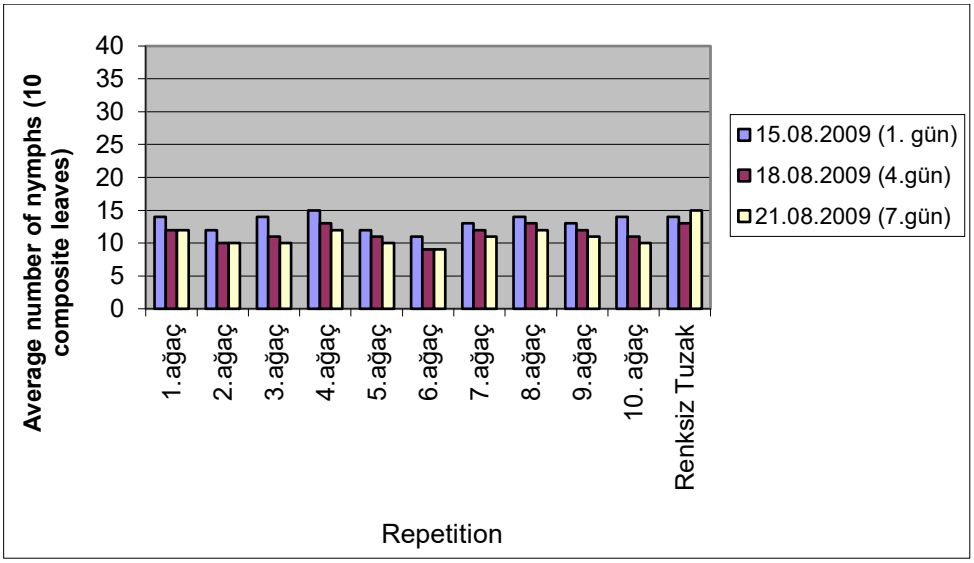

Figure 19. The effects of 4 (Four) hang trap application per tree on nymph population fluctuation of *Agonescena pistaciae* (between 13-17 nymph) on days 1st, 4th and 7th.

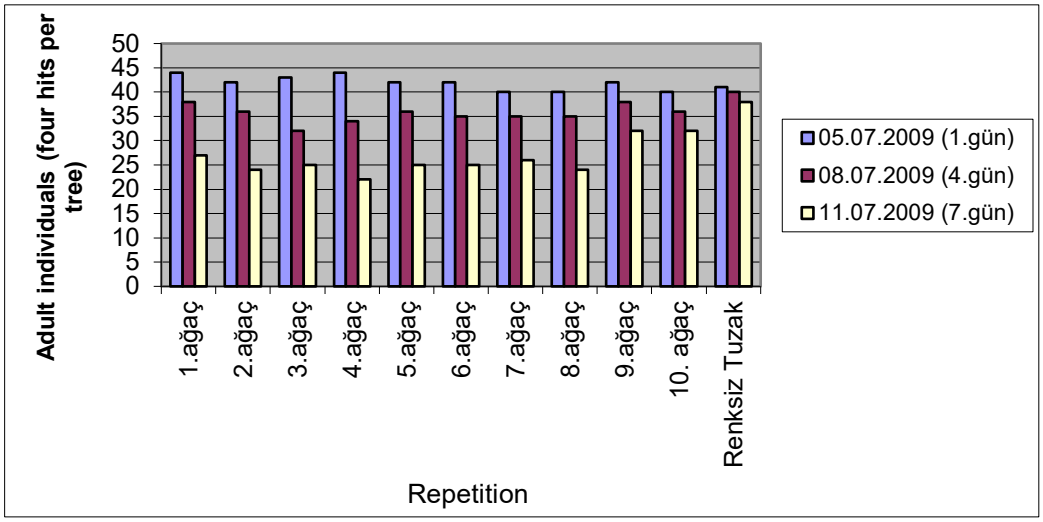

Figure 20. The effects of 4 (Four) hang trap application per tree on adult population fluctuation of *Agonescena pistaciae* (between 38-46 adults) on days 1st, 4th and 7th.

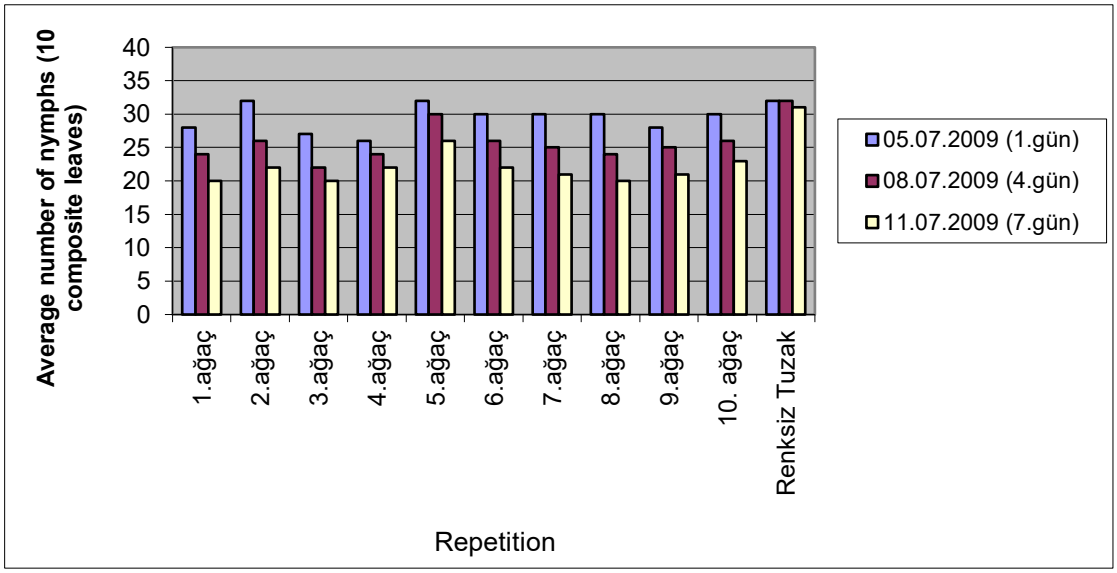

Figure 21. The effects of 4 (Four) hang trap application per tree on nymph population fluctuation of *Agonescena pistaciae* (between 28-37 nymph) on days 1st, 4th and 7th.

4 Discussion

Statistical analyses were performed in order to determine whether or not there are any differences between populations based on trap numbers, that is, whether or not the population increases or decreases with the increases in trap numbers and to determine whether or not number of traps affects the population size based on population type (adult or nymph) and based on increases in number of individuals in the population. The R^2 value was found as 85 in the analyses, and CV was 14. Results of analyses are given in Tables 10, 11 and 12.

No differences regarding densities were found between populations arising from hanging of traps. That is, the number of traps hung created reduction in populations in the same percentage whatever the density is (Table 10).

Table 10. Differences According to Population Densities.

Populations	Least Sq Mean
A	A .
B	A .
C	A .
D	A .

Counting the population in adults or nymphs did not create any differences in populations. There was parallelism between the adult and nymph counts on trees. Parallel results were obtained in nymph and adult trials whatever the number of traps hung were, showing the reliability of the studies (Table 11).

Table 11. Differences in Types of Populations (Biological Period)

Level	Least Sq Mean
Adult	A
Nymph	A

One of the significant assessments of the study involves the results created by the number of traps on populations. Based on the results of the study, populations tended to be higher in trees with 1 trap as compared to trees with 3 or 4 traps. Populations decreased with increasing numbers of traps, and results of this study were in parallel with the adult counts in traps. The adult population captured increased with the increasing number of traps, and this rate affected the nymph/adult populations on trees in different numbers (populations A, B, C and D) and populations decreased (Table 12). Again, as seen in the Table 12 below, different groups were obtained in trees with 3 or 4 traps hung.

Table 12. Evaluation of sticky trap numbers in terms of populations.

Level				Least Sq Mean
1	A			30,227273
3		B		26,060606
4			C	24,280303

In analyses aiming at determining if there are any differences between populations in the numbers of nymphs and adults, it was found that there were differences between the controls and other applications (Table 13).

Table 13. Populations in terms of nymphs and adults

Level				Least Sq Mean
11	A			29,666667
1	A	B		28,000000
2		B	C	27,611111
5		B	C	26,777778
7		B	C	26,555556
8		B	C	26,333333
3			C	26,222222
4			C	26,194444
9			C	26,111111
6			C	26,027778
10			C	25,916667

Acknowledgement: We are honored to submit our thanks to Daniel BUCKARD (Switzerland) for the identification of the species belonging to the Psyllidae family and to Republic of Turkey Ministry of Agriculture and Forestry General Directorate of Agricultural Research and Policies (TAGEM) for project support.

References

Altın, M., A. Yücel, H. Bolu, 1992. Güneydoğu Anadolu Projesi (GAP) Bölgesi Antepfıstığı Alanlarında Entegre Mücadele Çalışmaları Öncesinde Zirai Mücadelenin Gerçek Durumu, Karşılaşılan Sorunlar ve Çözüm Yolları. Uluslararası Entegre Mücadele Sempozyumu Bildirileri, 15-17 Ekim, İZMİR, S. 87-95.

Altın, M., Bolu, H. ve C. Kaplan, 1996. Güneydoğu Anadolu Bölgesi Antepfıstığı (Pistacia vera L.) Alanlarında Önemli Bazı Zararlı ve Yararlı Türlerin Populasyon Değişimlerinin Belirlenmesi Üzerinde Araştırmalar. Tarım ve Köy İşleri Bakanlığı Tarımsal Araştırmalar Genel Müdürlüğü Yayınları Sonuç Raporu. Proje Kod No: BK/96/06/09/504.25 s.

Bolu, H., 2002. Güneydoğu Anadolu Bölgesi Antepfıstığı Alanlarındaki Böcek ve Akar Faunası Üzerinde Araştırmalar. Türk. entomol. derg., 2002, 26 (3): 197-208.

Özgen, İ., Ayaz, T., Mutlu, Ç. and H. Bolu, 2013. The Capture Effects of Yellow Stick Traps in the Different Wavelengths to the Adults of Agonescena pistaciae Burc. & Laut. (Hemiptera: Psyllidae) from Turkey. Mun. Ent. Zool. 8 (1): 486-492.

Hadian, A.R. and H. Seyedoleslami, 2001. Effiency of Yellow Sticky Board Traps and Limb Jarring in the Capture of Adult Pistachio Psylla ***Agonescena pistaciae*** burkhardt & Lauterer (Hom: Psyllidae). J. Sci. & Technol. Agric. & Natur. Resour., Vol 6. No:2.

Hirota, T., and Y. Kato, 2001, ınfluence of visual stimuli on host location in the butterfly, ***Eurema hecabe*.** Entomologia Experimentalis et Applicata 101**:**199-206

International Journal of Innovative Engineering Applications

Journal homepage: https://dergipark.org.tr/ijiea

SECURING VULNERABILITIES IN DOCKER IMAGES

Ahmet Efe*[1], Ulaş Aslan[2], Aytekin Mutlu Kara[2]

[1] *Internal Auditor at Ankara Development Agency, Turkey*

[2] *Yıldırım Beyazıt University, Department of Computer Science, Turkey*

Abstract

Review Paper

Docker is an alternative application development and publishing infrastructure tool to various virtualization environments such as Virtual box and the like. The most popular containerization platform is Docker which is the area where Docker images are run. Container is a lightweight contrasting option to full machine virtualization that includes exemplifying an application in a container with its own working condition. These two concepts, virtualization and containerization are competing in the cloud-based environments. When virtualization became the mainstream, VM security concerns was common. IT Security experts are discussing the potential weaknesses of a virtualized environment for a long time. In this paper, focusing on Docker container, its vulnerabilities and possible measurements against security concerns, we have provided information about assessment of risks and vulnerabilities of containerization and the main differences between these two concepts via vulnerability analysis.

Keywords: *Technology, Vulnerabilities, Dockers, Containers, Cloud computing security*

1 Introduction

Docker is a program that performs working framework level virtualization otherwise called containerization. Docker is essentially developed for Linux, where it utilizes the asset confinement properties of the Linux, for example, cgroups and portion namespaces, and an association skilled record framework to permit free "containers" keeping in mind the end goal to keep running inside a solitary Linux occurrence, staying away from the overhead of beginning and keeping up virtual machines (VMs). Container-based virtualization uses single kernel to run multiple instances on an operating system and virtualization layer runs as an application within the operating system. It is also called operating system virtualization and in this approach, the kernel of operating system runs on the hardware node with different isolated guest virtual machines (VMs) called containers. [1]

Docker is an open source virtualization platform for software developers and system builders. With Docker you can run Linux and Windows virtual containers (machines) on Linux, Windows and MacOSX. With this platform, you can easily install, test and deploy web systems. The Docker takes the image of the software's installed state (such as an .iso DVD image) and makes it available again. If you wish, you can create this image once and send it to the servers you want, if you do not, then you will create an image from scratch on each server. Each server can reconstruct the same image by looking at the instruction files called the Dockerfile. There is no need for manual intervention.

As is depicted in the Fig 1, the structure development at Docker systems, depends on the Moby Project upon which ConteinerD, LinuxKit and İnfraKit have been used. Therefore, the Docker is developed by the Moby Project.

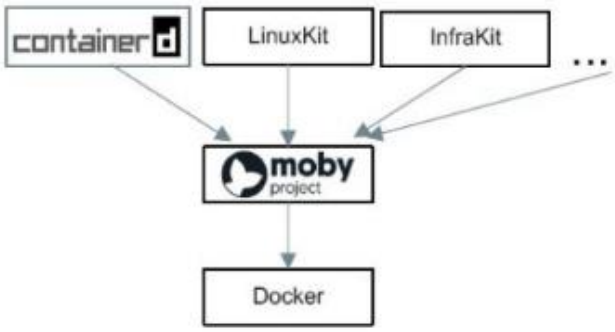

Figure 1 Development of Docker [2]

Docker is an apparatus that makes it simpler to make and run applications by utilizing container. Docker enables an engineer to bundle up an application with the greater part of the prerequisites, for example, libraries conditions and do everything as one bundle. By doing this, the engineer can rest guaranteed that the application will take a shot at some other Linux machine without depending of any altered settings that machine may have that could contrast from the machine utilized for composing and testing the code [3]. As is depicted in the Fig. 2, the usage of container technology will likely looks very different in ten years than they do now. Currently, containers are predominantly being used within the software development arena. Platforms such as Docker (the most mature of the container environments) are growing at exponential rates and taking nearly all market shares. Fig. 2 shows the rapid growth rate of Docker [4].

∗ Corresponding author.

E-mail address: icsiacag@gmail.com (A. Efe) | ORCID Number : *0000-0002-2691-7517*

Received 9 September 2019; Received in revised form 2 December 2019; Accepted 30 April 2020

 Doi: https://doi.org/10.46460/ijiea.617181

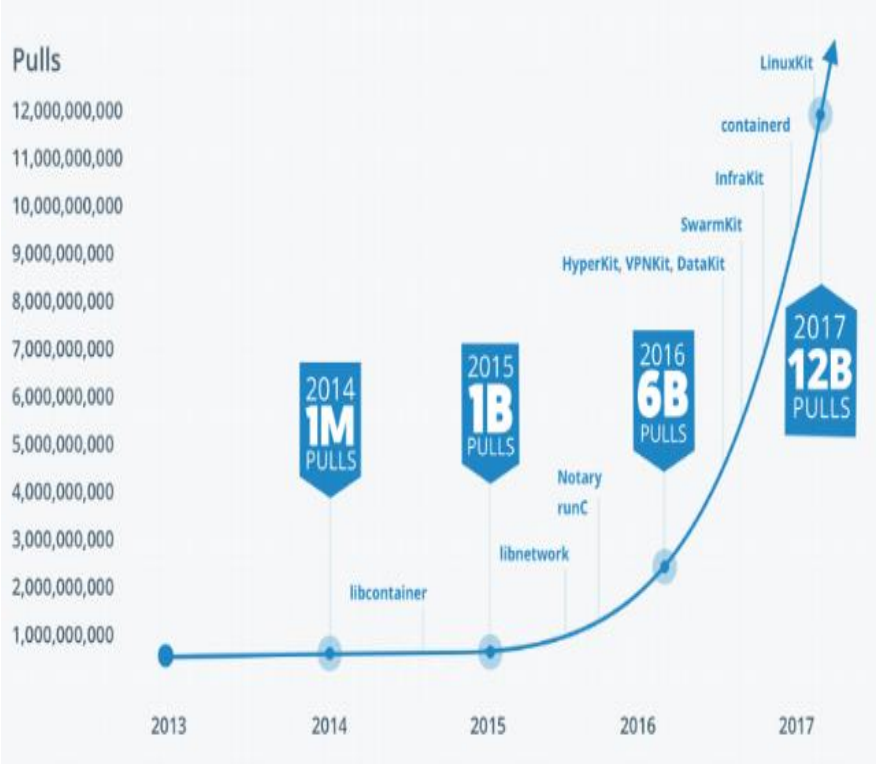

Figure 2 Growth rate of Docker [4]

2 Security Problems in the Docker Literature

Security studies on Docker platforms are still developing. In a study conducted by Bui, container-based virtualization is considered to be able to provide a more lightweight and efficient virtual environment, but not without security concerns. He analyzed the security level of Docker, a well-known representative of container-based approaches considering just two areas: the internal security of Docker, and how Docker interacts with the security features of the Linux kernel, such as SELinux and AppArmor, in order to harden the host system. He proposed that the security level of Docker containers could be increased if the operator runs them as "*non-privileged*" and enables additional hardening solutions in Linux kernel, such as AppArmor or SELinux [5].

In an analysis done by Combe *et al*, [6] it is revealed that Docker usages have security implications for both containers and their hosts, and repositories. Basics at al [7] have proposed that in order to increase Docker security and flexibility, an extension to the Dockerfile format to let image maintainers ship a specific SELinux policy for the processes that run in a Docker image, enhancing the security of containers is required.

Shu *et al*. [8], who have studied 356,218 docker images, made the following findings: (1) both official and community images contain more than 180 vulnerabilities on average when considering all versions; (2) many images have not been updated for hundreds of days; and (3) vulnerabilities commonly propagate from parent images to child images. They have proposed a scalable Docker Image Vulnerability Analysis (DIVA) framework for automatically discovering, downloading, and analyzing vulnerabilities in images from Docker Hub.

Manu *et al*, have provided unified security and privacy multilateral security architecture for cloud services stack, using key latest technology via LxC in general and Docker containers in specific to help assess the security design and architecture quality using multilateral security framework for Docker container. [9]. They have made a deep dive of the PAAS security and also try to analyze, compare and contrast the PAAS Docker container security, with other container technologies, and also with Virtual machine security with and without Hypervisor, and current security level of Dockers container[10]. Chelladhurai *at al*, have proposed security algorithms and methods to address DoS attacks related issues in the Docker container technology in their study [11].

Gao *et al*, discussed the root causes of the containers' information leakages and propose a two-stage defense approach [12]. According to Jian, who has searched defense methods against escape attack, Docker is faced with the risk of attacks that exploit kernel vulnerability by malicious users, once the exploit program in the container launches an effective escape attack can gain root privilege of the host, which will affect the reliability of other containers and the entire system [13].

3 Problem Definition and Methodology

There are many advantages of Docker (or container) technologies. However as Cyber security is a top concern in nearly every major industry, in Docker technology it is also the most controversial topic. Millions of web applications which run on Docker platform are open for cyber-attack. Since the time of Docker's release in 2013, several vulnerabilities have been discovered.

We used Docker and related technologies not only development environment but also production for many projects. We have faced with some problems and search for suitable solutions. All problems and solutions were documented and published in the company for the future use. The recommendations in this paper were collected from these experiments.

This paper focuses on the security threats of web applications. We explore current situation and several vulnerabilities. We suggest a new method to help increase security for the most common vulnerabilities. In order to research and suggest new methods, firstly we need to clarify the problems so that we can work on a much more specific area. In the below you can see some problems that we need to find a way to improve;

- How to analyze the security vulnerabilities of Docker system?
- What are the most commonly found vulnerabilities in Docker systems?
- How to detect vulnerabilities of a Docker system?
- How to detect and prevent DoS attacks on Docker?
- How to detect vulnerabilities in Docker images?

In this research, there are many methodologies combined to give more clear and whole explanations about the subject. In this paper, Literature review is the most crucial methodology. Because we have tried to see as much as many papers about this subject to observe what is done and what can be done about Docker Security. We try to give descriptions about docker and docker security. This paper is also a qualitative research paper due to the fact that we used the knowledge based on experience and observation that is obtained in the past researches that we review in order to make assumptions.

4 Working Structure of Docker Dynamics and Its Benefits

Developers can bundle their development environments into these containers with the necessary configurations and transfer them to the desired environment. This structure inspired by sea transport removes many problems from the point of view of both developers and system administrators. Docker leverages the resource isolation features of Linux to create a segmented, virtual environment that applications can operate on it. This is conceptually like using a tool like "*chroot*" to create an isolated, protected filesystem, although the segmentation under Docker extends beyond filesystem isolation alone to circumscribe resources. Below, there are the three main functions of the Docker platform:

- *Build*—Docker allows you to compose your application from microservices, without worrying about inconsistencies between development and production environments, and without locking into any platform or language.
- *Ship*—Docker provides developers to setup the whole software development steps such as development, testing, distribution and with a consistent user interface.
- *Run*—Docker provides developers the ability to deploy scalable services securely and reliably on a wide variety of platforms.

Docker has three main parts:

- *Docker Engine*; Open-source containerization platform
- *Docker Cloud;* including Docker Hub; Software as a Service (SaaS) platform for sharing and managing Docker containers
- *Docker Datacenter*; On-premise solution for sharing and managing Docker containers and Docker-containerized applications.

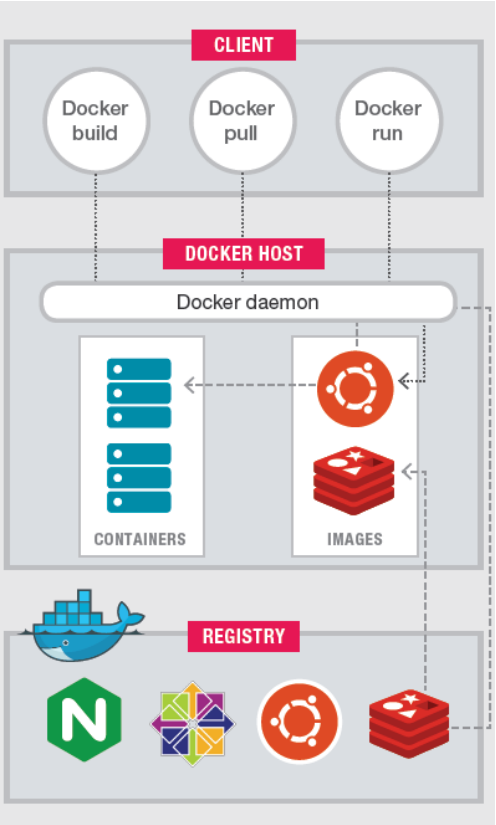

Figure 3. Docker Architecture [15]

Docker uses client-server architecture. The Docker client tells the Docker daemon, which is on the host operating system and builds, runs and distributes containers. Docker users communicate with the daemon through the client, which is the Docker binary. In the figure, Docker architecture is shown. [16]

Users are always expecting applications to available, elastic, scalable and interoperable at any time. Docker provides these features to users. Main benefits of Dockers are;[17]

Docker containers are negligible: Containers has one or only a couple of running procedures. Less programming implies littler likelihood of being influenced by helplessness.

Docker containers are task-particular: There is a pre-meaning of what precisely ought to keep running in the containers, way of the information indexes, required open ports, daemon arrangements, mount focuses, and so forth. Any security-related oddity is less demanding to identify than in other multi-reason frameworks.

Docker containers are segregated: It is disengaged both from the facilitating framework and from different containers.

Docker containers are reproducible: Due to their explanatory form frameworks any administrator can without much of a stretch assess how the holder is manufactured and completely see each progression. Based on various evaluation and experiments, Docker provides fast deployment, small footprint and good performance which make it potentially a viable Edge Computing platform [18].

Let us express the difference between other virtualization technologies and Docker in a simple example. For example; An Ubuntu operating system will be installed. To perform this operation on other virtualization technologies, an Ubuntu version must have an ISO file. In the Docker structure, it is enough to write the command:

docker pull ubuntu

This command will install all versions of Ubuntu on the Docker repository. In other virtualization technologies, it is necessary to download and install the ISO file for each version, which causes more time loss. Docker operations are carried out via the terminal. Some interfaces have been developed to make our operations even easier with Docker. Using these interfaces we can manage our containers even more easily [19].

5 Comparison with VM Structures

Containers are less adaptable contrasted with VM's, MS windows, can't be keep running on a Linux OS, Containers are less secure contrast with VM, because of containers keep running in tight coupling with have OS and keeps running over it, if the container is traded off then hacker/assailant can get finish access to have OS and assets, additionally it is perplexing to introduce, setup the earth, oversee, direct, and automate the framework utilizing Container innovation. Container base virtualization utilizes have OS level virtualization, so framework security is of most extreme significance to screen utilizing the multilateral adjusted security Containers are executed in client space on peak of an OS piece.

- *Virtual Machines*

Each virtual machine includes the application, the necessary binaries, libraries, and an entire guest operating system — all of which may be tens of GBs

- *Containers*

Containers include the application and all of its dependencies but share the kernel with other containers. They run as an isolated process in user space on the host operating system. They are also not tied to any specific infrastructure — Docker containers run on any computer, on any infrastructure and in any cloud [16].

6 Docker Vulnerabilities

Since Docker's release in 2013, there has been discovered several vulnerabilities that could lead to privilege escalation code execution. Here in the below there are top five vulnerabilities that found different versions of Docker.

1. *CVE-2014-9357*

This vulnerability was identified in Docker Version 1.3.2 which allowed the execution of arbitrary code with root privilege. During the decompression of LZMA (.xz) archives, there was privilege escalation vulnerability. This vulnerability was patched by version 1.3.3.*26* **(CVSS Score: 10.0)** [23]

2. *CVE-2014-6407*

This vulnerability was identified in Docker Version 1.3.1, which allowed privilege escalation through symlink, and hard link traversals found in the Docker's image extraction. This vulnerability was patched by version 1.3.2.*27* **(CVSS Score: 7.5)** [24].

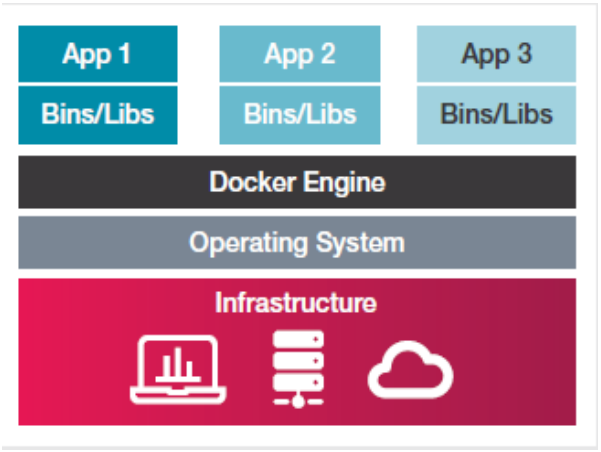

Figure 4 Container Architecture [17]

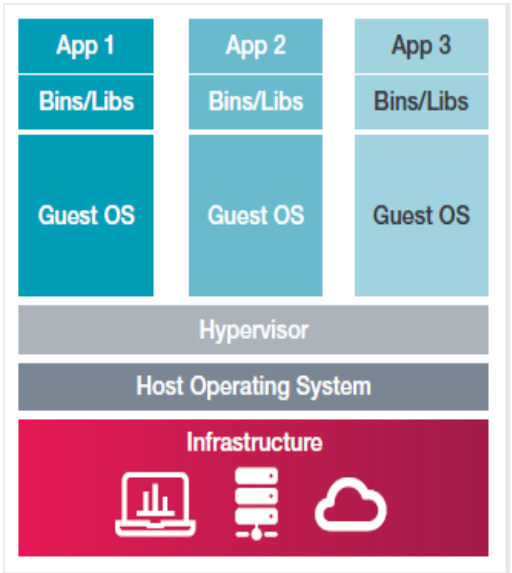

Figure 5 VM Architecture [15]

3. *CVE-2014-3630*

This vulnerability was identified in Docker Version 1.6.0 and allowed attackers to bypass security due to weak permissions on the /proc paths. Attackers could access sensitive information and perform unauthorized actions due to the security bypass. This vulnerability was patched by version 1.6.1.*28* **(CVSS Score: 7.2)** [25]

4. *CVE-2014-3499*

This vulnerability was identified in Docker 1.0.0 which indicated that Docker was using "world-readable" and "world-writable" permissions on the management socket. This vulnerability allowed local users to gain root

privileges to the local machine. This vulnerability was patched by version 1.0.1.*29* (CVSS Score: 7.2) [26]

5. CVE-2015-3627

This vulnerability was identified in Docker 1.6 and the Libcontainer version 1.6.0 that allowed a "mount namespace breakout" when a container was respawned. This function created an exploit to allow codes to escape the container. Through this exploit, attackers can create a privilege escalation. This vulnerability was patched in Docker 1.6.1. (CVSS Score 7.2) [27]

There are some specific parts of Docker hub contains both official and community images. Official Docker based architectures, which are more prone to attacks. Some of them are related to the images. Docker distributes applications in the form of images. Each image contains the target application software as well as its supporting libraries and configuration files. Repositories contain public, certified images from vendors. In contrast, any user or organization can create community repositories. [15] Some further vulnerability is related to the Docker architecture. [17]

If any attacker compromises host system, the container isolation and security safeguards will not make much of a difference. Besides, containers run on top of the host kernel by design. The kernel is shared among all containers and the host, magnifying the importance of any vulnerabilities present in the kernel. Should a container cause a kernel panic, it will take down the whole host [14].

An attacker who gains access to a container should not be able to gain access to other containers or the host [14.] The "container breakout" term is used to denote that the Docker container has bypassed isolation checks, accessing sensitive information from the host or gaining additional privileges.

Containers are much more numerous than virtual machines on average, they are lightweight, and you can spawn big clusters of them on modest hardware, but it implies that many software entities are competing for the host resources. If one container can monopolize access to certain resources, it can starve out other containers on the host, resulting in a denial-of-service (DoS), whereby legitimate users are unable to access part or all of the system. [14]

Docker's popularity is since, with containers, anybody can bundle code and conditions into a picture and distribute effortlessly to a registry whenever anywhere. From there, anybody can download the picture and run containers from the picture. This has brought convey ability of code crosswise over groups and stimulated the application lifecycle.

However, containers can incidentally uncover vulnerabilities, if the required precautions are not taken. This is particularly obvious when working with container images that are shared amongst clients and associations. Container images are downloaded from registries like Docker Hub or outsider registries. There are official and unauthorized repositories. These registries contain a large library of images. These registries are mainly user created and uncontrolled, this leads to low frequency of updates which results in vulnerabilities in the images.

A few examinations demonstrate that over 30% of authority repositories contain images that are insecure to an assortment of security assaults [21].

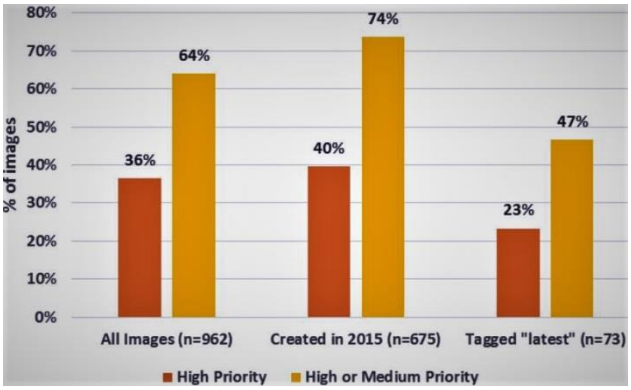

Figure 6 Official Image Vulnerabilities [21]

Fig 6 demonstrates the primary outcomes got by breaking down every official image from Docker Hub. In excess of 33% of all images have high need vulnerabilities and near 66% have high or medium need vulnerabilities [21].

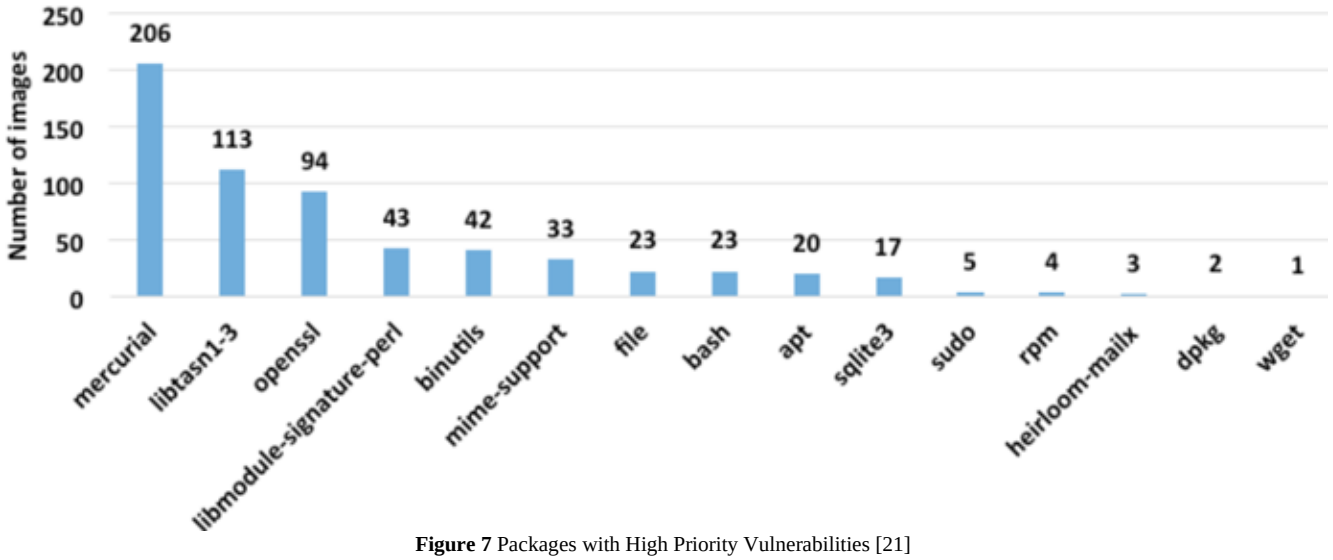

Figure 7 Packages with High Priority Vulnerabilities [21]

The as of late discharged powerlessness in inconsistent is available in a huge part of images (~20%). Prominent OpenSSL vulnerabilities, for example, Heartbleed and Poodle are available in near 10% of authority Docker Hub images [21].

Fig. 8 demonstrates the fundamental outcomes after breaking down general images. Generally speaking, the level of vulnerabilities is essentially higher than that of Official images [21].

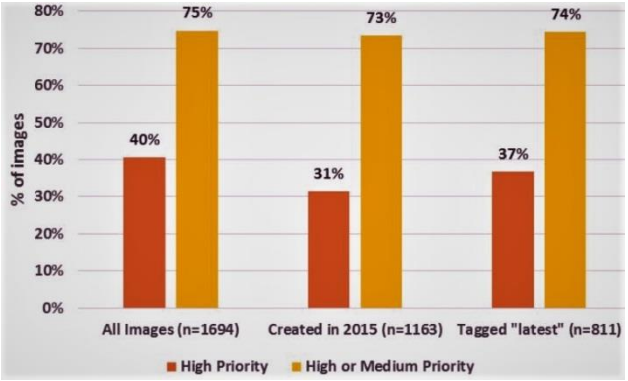

Figure 8 General Image Vulnerabilities [21]

According to a security analysis report released by a researcher from Federacy, 24% of images in public repositories were found to have significant vulnerabilities, with around 11% among them rated high, 13% as moderate and the rest as potentially vulnerable. [22]

Docker Hub, one of the cloud-based Docker container libraries, has been compromised by data spoofing by an unknown attacker by accessing the company's only Hub database in 2019. Docker Hub is an online repository service where users and organizations can create, test, store and distribute Docker container images both publicly and privately. It was reported that sensitive data were generated for approximately 190,000 Hub users, including the Github and Bitbucket markers for a small percentage of the affected users, as well as user names and hash codes for Docker repositories. Docker Hub has sent information e-mails to affected users, providing information about the security event and suggesting that they change their passwords to their online accounts using the same password for Docker Hub. Docker Hub said that the company will continue to investigate security breaches and will share more information whenever possible. The company is also working to improve its overall security processes and review its policies following violations. [30]

7 Possible Measures and Precautions Against Risks and Threats

Some security analysis tools can be used to inspect public Docker images. Security audit, container image verification, runtime protection, automated policy learning or intrusion prevention capabilities can be tested using these tools. Anchore Navigator, AppArmor, AquaSec, BlackDuck Docker, Cavirin, Cilium are some tools that can be used to analyze container security.

7.1. Checking the source of images

Container images are downloaded from registries like Docker Hub or outsider registries like Quay. These registries have Container images from associations and people alike. The same number of as official stores from IT merchants, there are numerous unapproved repositories too. Over the application lifecycle, designers, QA and IT will download numerous images for various sorts of purposes. It's vital to screen these images and play out a few controls previously they are introduced.

In order to do this, Docker Content Trust can be enabled, which integrates with third-party registries to verify digital signatures for container images that are downloaded from them. This helps developers to make whitelist of official repositories from authorized, trusted sources.

In the event that it is expected to work with unsubstantiated images from accomplices and sellers, for instance, it could be considered updating your images checking to heartier container security devices like Twist bolt. It filters images, as well as gives you a chance to set up custom cautions at whatever point anybody endeavors to introduce suspicious images.

7.2. Implementing powerful access controls

The wellspring of container images and use of official images can leave images traded off. Along these lines, get to control is to a great degree critical for holder pictures.

Normally, all clients are doled out root benefits inside a container. In any case, this is not the best practice from the security perspective. At whatever point a client is made, you have to change their entrance level to non-root. Certain clients will in the long run require root access to finish certain undertakings, however these special cases ought to be made just inside those compartments that play out the assignment, and just on the off chance that it is important. This undertaking driven access control guarantees that regardless of whether one client account is traded off, assailants cannot make much harm on whatever is left of the framework. It is unrealistic to physically change the status of clients for each container unfailingly. This errand should be robotized. A stage like Twistlock empowers role-based access control (RBAC) for pictures, and gives you a chance to obtain benefits to clients in light of their activity work. You can arrange RBAC in view of complex decides and guarantee that all clients have the vital benefits to do their undertakings nothing less, and nothing more.

7.3. Keeping containers lightweight

Engineers are attracted in to containers because of the lighter structure contrasted with virtual machines (VMs). When running containers, it's conceivable to stack an excessive number of bundles on a container with the goal that it progresses toward becoming enlarged to in excess of 100 MB. The perfect container size ought to be only several MBs.

While choosing an OS for your image's base layer, search for a moderate choice. There are two or three great choices like BusyBox, Alpine Linux, and RancherOS. Furthermore, introduce just the bundles that are required for a container to play out its undertaking. This enhances

the execution of containers, and critically, diminishes the assault surface territory.

7.4. Keeping images solid

Once you have taken after every single best practice to set up your images the correct way, it is essential to screen their wellbeing amid runtime. This requires routine "wellbeing checks" on the holders. On the off chance that Docker Engine discovers containers that are not working, it can naturally supplant them. Along these lines, you can keep the framework sound regardless of whether singular containers are observed to be helpless.

A critical practice to guarantee the great strength of your containers is to keep container images refreshed with the most recent form and apply security patches to them as often as possible. You should have the capacity to filter the images amid runtime to discover vulnerabilities and fix them expeditiously.

Identifying vulnerabilities is not a simple undertaking, as your framework could run a huge number of containers. At this scale, you require a risk discovery instrument like Twistlock that screens container runtime with the assistance of machine learning calculations. It can spot concerning examples and alarm you on their effect. This activity of finding the needle in the pile is not conceivable through manual poring over of log information and measurements—it takes wise calculations and a cutting-edge risk discovery stage like Twistlock.

7.5. Handling secret information with mind

In spite of doling out read-just access to clients, despite everything you have to watch what information stored in your containers. For instance, you ought to never store confidential information like passwords, tokens, keys, and private client data inside docker documents. Regardless of whether erased later, this information can be recovered from the image's history. Rather, you should utilize the privileged insights administration highlight that accompanies both Kubernetes and Docker Swarm. Every one of them have solid defaults to guarantee security credentials are appropriately scrambled, put away in an encoded design, and when recovered, can be decoded just by approved clients.

Holder images are likely the best time some portion of the Docker encounter. However, they can likewise be the most perilous from a security outlook. By understanding the different subtleties to Docker image security, you can guarantee your cloud-local applications are considerably more secure than your heritage applications ever were. [20]

8 Conclusions

Development environments can vary from project to project. Even the installations of the same project with different customers contain different components. It may take a lot of time to install the same environment in the developer environment in order to solve the problems of the customers. Some software houses maintain developer environments on virtual servers in order to repeat installations in developer environments in different versions with different customers. Considering that a virtual machine is around 25 GB on average, if a single project is installed on 5 customers, 125 GB of space will be required on each developer's computer. Even if we ignore the problem created by the provision of virtual servers in resource usage, in every projects that are actively developing, web server changes, database schema or reference data changes, etc., the distribution of the master virtual machine in binary format to all developers, and if any, it requires the developers to apply their own customizations to these machines again and again. Another development environment problem is the time spent in setting up the computers of newcomers with the necessary tools in development environments where no virtual server is used. This is usually done by an experienced senior member of the team, in which case a period of time that both the experienced member of the team and the new member can effectively use is lost.

Cloud computing makes extensive use of virtual machines because they permit workloads to be isolated from one another and for the resource usage to be somewhat easily controlled [28]. Docker is an open platform for developers and system administrators to build, ship, and run distributed applications using Docker Engine, which is a portable, lightweight runtime and packaging tool, and Docker Hub, which is a cloud service for sharing applications and automating workflows. The main advantage is that, Docker can get code tested and deployed into production as fast as possible [29].

Since the Docker was introduced to the market, a series of updates and changes have been made to improve its functionality and security. However, as any programmer knows, there is no safe platform and for the Docker there is also no exception. Also, most of the time, security is affected by how a user interacts with the Docker, which faces several problems with human errors. In a study of more than 700 companies from many developed countries conducted by Cloud Foundry in 2016, half of the companies used the container technology. Of these, 64% plan to expand the use of container technology. When we look at this rapid increase in container usage, new security problems are constantly emerging. The more a system is used by users, the more it becomes a strategic target for attackers. The Docker seems to be the most widely used container technology today, and as with many other similar platforms, many have protocol-specific security issues. A list of weaknesses previously found in the Docker can be viewed on CVE-List and information about these security issues can be found.

Cyber Security is at the forefront of today's data centers and for good reason. Even a very small-scale violation can lead to very large damage. For this reason, organizations need to be particularly sensitive to security implications and new security vulnerabilities. When virtualization became the mainstream, VM security was common. IT Security experts are discussing the potential weaknesses of a virtualized environment for a long time.

Perhaps the worst case scenario is "*VM Escape*". This term is used to describe a situation in which an attacker can endanger a guest virtual machine and be "escaped" from within the virtual machine and access other main operations on the hypervisor. Virtualization leaders have made great efforts to ensure that such security issues are addressed, and the VM escape is rejected as a real threat. A weakness called "*CEN-2015-*

3456" and "*VENOM*", and by exploiting some of the vulnerable codes in QEMU's virtual floppy drive, the attackers potentially had the advantage to exploit other virtual machines running on the host computer. For this reason, the Docker can help with container security, even if it is not a virtualization service.

From Docker 1.8 version, a new security feature called "*Docker Content Trust*" has been introduced. This feature allows verifying the authenticity, integrity and releasing date of all Docker images in the "Docker Hub" repository. This content assurance is not enabled by default. When enabled, Docker cannot download any of the unsigned images and therefore becomes more secure.

To enable this feature:

sudo export DOCKER_CONTENT_TRUST = 1.

The Docker will inform when trying to download an image that is not already signed. By default, there is no resource constraint in a container, and the host can use most of the given resource to the extent allowed. The Docker provides a way to control the amount of memory, CPU, or block that the container run command can use. It is possible that when a container runs into trouble and starts consuming all of the host's resources, bad results may occur on a scenario. The resource limits for containers can be set from the "*docker run*" command for further security considerations.

References

[1] Singh, S., Singh, N. "Containers & Docker: Emerging roles & future of Cloud technology", 2nd International Conference on Applied and Theoretical Computing and Communication Technology (iCATccT), 16850813 DOI: 10.1109/ICATCCT.2016.7912109, IEEE, 21-23 July 2016.

[2] Morgan, T. P. "Docker Completes Its Platform Wıth Dıy Lınux" 2017.

[3] What is Docker? (n.d.). Retrieved from URL: https://opensource.com/resources/what-docker

[4] Docker. (n.d.). Retrieved from Docker Website URL: https://www.docker.com/

[5] Bui, T., "Analysis of Docker Security" Aalto University T-110.5291 Seminar on Network Security, 2014.

[6] Combe, T., Martin, A., Pietro, R.D. "To Docker or not to Docker: a security perspective" IEEE Cloud Computing, 2016.

[7] Bacis E., Mutti, S. Capelli, S. Paraboschi, S. "DockerPolicyModules: Mandatory Access Control for Docker containers" IEEE Publishing, 2015.

[8] Shu, R., Gu X., Enck, W., "A Study of Security Vulnerabilities on Docker Hub" CODASPY '17 Proceedings of the Seventh ACM on Conference on Data and Application Security and Privacy, 2017.

[9] Manu, A R, Patel, J. K., Akhtar S., Agrawal, V. K., Murthy K N, "Docker container security via heuristics-based multilateral security-conceptual and pragmatic study", IEEE Publishing, 2016.

[10] Manu, A R, Patel, J. K., Akhtar S., Agrawal, V. K., Murthy K N, "A study, analysis and deep dive on cloud PAAS security in terms of Docker container security", International Conference on Circuit, Power and Computing Technologies (ICCPCT), 2016.

[11] Chelladhurai, J., Chelliah, P., Kumar, S. A., "Securing Docker Containers from Denial of Service (DoS) Attacks" International Conference on Services Computing (SCC), 2016.

[12] Gao X., Gu, Z. Kayaalp, M., Pendarakis, D., Wang, H., "ContainerLeaks: Emerging Security Threats of Information Leakages in Container Clouds" 47th Annual IEEE/IFIP International Conference on Dependable Systems and Networks (DSN), 2017.

[13] Jian, Z., Chen, L.,"A Defense Method against Docker Escape Attack" ICCSP '17 Proceedings of the 2017 International Conference on Cryptography, Security and Privacy, 2016.

[14] Five Security concerns when using docker. (n.d.). Retrieved from Oreilly URL: https://www.oreilly.com/ideas/five-security-concerns-when-using-docker

[15] Rui, S., Xiaohui, G., & William, E. A Study of Security Vulnerabilities on Docker Hub. CODASPY '17 Proceedings of the Seventh ACM on Conference on Data and Application Security and Privacy (pp. 269-280). Scottsdale, Arizona, USA: ACM. March 22 - 24, 2017.

[16] ISACA, Understanding the Enterprise Advantages of Application Containerization. (n.d.). USA. 2016.

[17] Docker Security Vulnerabilities. (n.d.). Retrieved from Sysdig URL: https://sysdig.com/blog/7-docker-security-vulnerabilities/

[18] Ismail B. I. et al., "Evaluation of Docker as Edge computing platform," 2015 IEEE Conference on Open Systems (ICOS), Bandar Melaka, 2015, pp. 130-135.doi: 10.1109/ICOS.2015.7377291

[19] Ayaz Ö., Aydın G., "Uygulama Sanallaştırmada Yeni Bir Yaklaşım: Docker", URL: https://ab.org.tr/ab15/bildiri/312.pdf

[20] Twistlock. (n.d.). Retrieved from 5 Best Practices to Container Image Security: https://www.twistlock.com/2017/08/31/container-image-security-best-practices/

[21] Over 30% of Official Images in Docker Hub Contain High Priority Security Vulnerabilities. (n.d.). Retrieved from banyanops URL: https://blog.banyansecurity.io/blog/over-30-of-official-images-in-docker-hub-contain-high-priority-security-vulnerabilities

[22] Federacy. (n.d.). Retrieved from Container Scanning Specification URL: https://www.federacy.org/docker_image_vulnerabilities

[23] Docker 1.3.3 Security Advisor. Retrieved from Security focus Website URL: https://www.securityfocus.com/archive/1/archive/1/534215/100/0/threaded

[24] Bug 1167505 - (CVE-2014-6407) CVE-2014-6407 docker: symbolic and hardlink issues leading to privilege escalation. Retrieved from bugzilla.redhat Website URL: https://bugzilla.redhat.com/show_bug.cgi?id=1167505

[25] SUSE-SU-2015:0984-1: moderate: Security update for docker.Retrieved from Suse Website: http://lists.suse.com/pipermail/sle-security-updates/2015-June/001419.html

[26] RHSA-2014:0820 - Security Advisory. Retrieved from redhat Website URL: https://access.redhat.com/errata/RHSA-2014:0820

[27] Docker 1.6.1 - Security Advisory [150507]. Retrieved from Seclists Website URL: http://seclists.org/fulldisclosure/2015/May/28https://www.cvedetails.com/vulnerability-list/vendor_id-13534/product_id- 28125/Docker-Docker.html

[28] Felter, W. Ferreira, Rajamony A. R. and Rubio, J. "An updated performance comparison of virtual machines and Linux containers," 2015 IEEE International Symposium on Performance Analysis of Systems and

Software (ISPASS), Philadelphia, PA, 2015, pp. 171-172. doi: 10.1109/ISPASS.2015.7095802

[29] Preeth E N, F. J. P. Mulerickal, B. Paul and Y. Sastri, "Evaluation of Docker containers based on hardware utilization," 2015 International Conference on Control Communication & Computing India (ICCC), Trivandrum, pp. 697-700.doi: 10.1109/ICCC.2015.7432984, 2015.

[30] Wei, W. “Docker Hub Suffers a Data Breach, Asks Users to Reset Password” 2019.

International Journal of Innovative Engineering Applications

Journal homepage: https://dergipark.org.tr/ijiea

A NEW RECORD FOR NITIDULIDAE FAUNA OF TURKEY: *SORONIA PUNCTATISSIMA* (ILLIGER, 1794) (COLEOPTERA: NITIDULIDAE)

İnanç Özgen*[1], Aykut Topdemir[1]

[1] *Fırat University, Faculty of Engineering, Department of Bioengineering, Turkey*

Abstract

Short Note

In this study; a widespread nitidulid species *Soronia punctatissima* (Illiger, 1794) is reported for the first time from Turkey.)

Keywords: *Soronia punctatissima, Nitidulidae, New record, Turkey*

1 Introduction

The Nitidulidae family is represented by around 4.000 species, which are included in the team of beetles (Coleoptera) and spread all over the world (Baviera & Audisio, 2014, Anlaş and Özgen, 2018). In Turkey, 215 species belonging to five subfamilies in the family Nitidulidae are reported. (Avgın et al., 2015). As for the genus Soronia Erichson, 1843, four species were listed. Including this record, five species of this genus is known from Turkey The studied material from East Anatolia was collected in the year 2013 from a mountain area and its banks. The samples were collected by shifter on soil and they were preserved in 70% ethanol. Specimens were identified by Eduard Khachikov (Russia).

Soronia punctatissima (Illiger, 1794)

2 Material examined

Turkey: Elazığ, Sivrice, Hazarbaba Mountain, 29.V.2013, 11 exs, 2.225 m, leg. Khachikov & Özgen.

3 Distribution in world

Austria, Belarus, Belgium, Bosnia and Herzegovina, Britain , Bulgaria, Central European Russia territory, Corsica, Crotia, Czech Republic, Denmark, East European Russia territory, Eastern Palearctic, Estonia, Finland, France, Germany, Hungary, Ireland, Italy, Latvia, Lithuania, Luxembourg, Moldova, Near East, North European Russia territory, Northern Ireland, Nortwest European Russia territory, Norway, Poland, Romania, Sardinia, Slovakia, Slovenia, South European Russia territory, Spain, Sweden, Switzerland, The Netherlands, Ukraine, Yugoslavia (Jelínek & Audisio, 2007).

In the future studies, the behavior of the species in the habitat should be determined.

4 References

Anlaş, S. and İ. Özgen, 2018. Türkiye Nitidulidae Faunasına Katkılar. Anadolu I. Uluslararası Multidisipliner Çalışmalar Kongresi, Tam Metin Kitabı, 28-29 Aralık, 2018, Diyarbakır. 967-969 s.

Baviera C. & Audisio P. 2014. The Nitidulidae and Kateretidae (Coleoptera: Cucujoidea) of Sicily: Recent records and updated checklist. Atti della Accademia Peloritana dei Pericolanti Classe di Scienze Fisiche, Matematiche e Naturali, Vol. 92, No. 2, A1, 32 pp.

Avgın, S. S., Antonini, G., Lason, A., Jansson, N., Abacıgil, T.Ö., Varlı, S.V., Biase, A.D. and P. Audisio, 2015., New data on distribution, ecology, and taxonomy of Turkish Nitidulidae (Coleoptera). Turk J. Zool , 39: 314-322.

Jelínek J., Audisio P. (2007). Family Nitidulidae. In: Löbl I, Smetana A, editors. Catalogue of Palaearctic Coleoptera. Vol. 4: Elateroidea - Derodontoidea - Bostrichoidea - Lymexyloidea - Cleroidea - Cucujoidea. Stenstrup, Denmark: Apollo Books, pp. 459–491.

∗ Corresponding author.

E-mail address: inancozgen@gmail.com (İ. Özgen) | ORCID Number : 0000-0003-1742-9324

Received 15 May 2020; Received in revised form 12 June 2020; Accepted 15 June 2020

2587-1943 | Doi: https://doi.org/10.46460/ijiea.737731